UNIVERSITÀ DEGLI STUDI DI PADOVA

Sede Amministrativa: Università degli Studi di Padova

Dipartimento TERRITORIO e SISTEMI AGRO-FORESTALI

Scuola di Dottorato di Ricerca in TERRITORIO, AMBIENTE, RISORSE E SALUTE. Indirizzo: ECOLOGIA - Ciclo XXII

THE EFFICIENCY OF XYLEM NETWORK IN TREES: A THEORETICAL AND EXPERIMENTAL APPROACH

Dottorando: Francesco Grani

Direttore della Scuola: Ch.mo Prof. M. A. Lenzi

Supervisore: Ch.mo Prof. Tommaso Anfodillo

Anno Accademico 2010

Riassunto

All'interno degli alberi, l'acqua si muove per mezzo di un gradiente negativo di pressione, che si instaura tra le radici e le foglie, attraverso una rete di cellule xilematiche la cui lunghezza può raggiungere l'ordine di grandezza di 100 metri nelle piante più alte del pianeta.

Questa imponenza del sistema di trasporto comporta la necessità da parte della pianta di porre in atto degli stratagemmi per far fronte alla crescente resistenza idraulica che si sviluppa assieme al drastico allungamento di percorso idrico durante tutta l'ontogenesi. Vale a dire che l'aumento in altezza delle piante è accompagnato da un conseguente aumento di resistenza idraulica all'interno dello xilema. La più efficace delle soluzioni per contenere questo aumento di resistenza idraulica sembrerebbe essere la rastremazione degli elementi di conduzione.

L'introduzione da parte del modello WBE (West, Brown, Enquist 1997, 1999) dell'ipotesi di universalità del grado di rastremazione dei condotti xilematici nelle piante vascolari, porta ad introdurre una soglia di rastremazione "ottimale" tale da rendere all'incirca costante la resistenza idraulica di un percorso a prescindere dalla sua lunghezza (potenzialmente sempre suscettibile di crescita). E' stato dunque ipotizzato che le limitazioni di natura idraulica alla crescita in altezza delle piante possano essere conseguenti all'insorgere di una sub-ottimalità del grado di rastremazione dei condotti proveniente dall'impossibilità fisica di aumentare indefinitamente il loro diametro alla base, od in alternativa che una sub-ottimalità generale del sistema di trasporto idraulico all'interno della pianta possa manifestarsi ad un certo punto dello sviluppo in altezza (e quindi in lunghezza ed in volume dei condotti xilematici) in conseguenza alla non possibilità di mantenimento di uno stato d'equilibrio ottimo del sistema di conduzione, pensato come una rete di trasporto ottimizzata (Banavar, Maritan, Rinaldo 1999) in cui il volume di servizio presente all'interno della rete e la resistenza idraulica conseguente allo spostamento di tale volume, siano entrambi minimizzati in una logica di soluzione d'equilibrio di minimo vincolato.

Uno degli obiettivi di questo lavoro è stato mettere assieme due dei principali modelli recentemente proposti all'attenzione della comunità scientifica (il modello WBE ed il modello BMR) e di raccogliere nello sviluppo di un nuovo unico modello di scala le ipotesi e le intuizioni principali dei due, per cercare di dare una risposta alla domanda fondamentale sott'intesa in questo argomento di ricerca: "per l'insorgenza di quali fattori le piante smettono di crescere in altezza?".

Nella prima parte viene presentata una breve ma sufficientemente approfondita analisi delle ipotesi del modello WBE e del modello BMR, mostrando i passaggi principali che portano ai risultati racchiusi nei due modelli, ed i risultati stessi. All'interno dello stesso capitolo viene quindi dato spazio al modello proposto da questa tesi, nel quale si risolve un problema di minimo vincolato in cui, scelto un condotto di tipo *powerlaw shape* (aderente alle ipotesi del modello WBE e non in contraddizione con le ipotesi sulla rete di trasporto contenute nel modello BMR), questo condotto viene realizzato con una variazione continua di forma passando dalle due condizioni di soluzione estreme ed opposte tra loro tipiche l'una della soluzione di minima resistenza del percorso (un cilindro) e l'altra della soluzione di minimo volume di servizio contenuto (un tronco di cono), alla ricerca della soluzione di migliore compromesso. Vengono quindi analizzate le motivazioni per cui non è possibile giungere ad una soluzione matematica in forma chiusa del problema posto, e si rende quindi necessario lo sviluppo di un modellino software per la risoluzione del modello. Al termine, viene mostrata la soluzione proposta dal nostro modello, ottenuta anche a partire dall'input di dati reali di piante, convergenti tutti ad una unica soluzione stabile di ottimo vincolato.

Successivamente a questa prima parte viene descritto lo svolgimento di un esperimento di riscaldamento dei getti apicali di alberi di treeline attraverso cui si discute l'importanza della rastremazione degli elementi di conduzione in specie di conifere (*Pinus cembra, Larix decidua* e *Picea abies*) ed in particolare del getto apicale che viene sottratto con un meccanismo di riscaldamento localizzato alle basse temperature di cui si dimostrano così le importanti conseguenze sulla limitazione alla crescita in altezza.

L'esperimento descritto nel secondo capitolo e condotto lungo due stagioni vegetative, ha dato modo di riflettere sulle caratteristiche ottimali che deve avere la strumentazione impiegata in campo ed in particolare sull'utilità di disporre di dispositivi di acquisizione dati efficaci, economici ed affidabili, eventualmente modulari e riprogrammabili secondo le necessità.

Nell'ultima parte viene quindi presentata la progettazione e la realizzazione di un sistema di datalogging basato sulle filosofie del software libero. In parallelo alle altre attività di ricerca esposte infatti gli ultimi due anni sono stati impiegati anche per la realizzazione di un sistema di acquisizione di dati basato sulla piattaforma hardware open source Arduino, rivolto in particolare al datalogging di sensori di tipo Granier per la misura di flusso di linfa nelle piante.

Il datalogger realizzato offre numerosi vantaggi rispetto alle soluzioni proposte dalle maggiori aziende che operano nell'acquisizione di dati in campo scientifico. A prescindere dalla notevole economicità del sistema progettato infatti, la precisione offerta nella conversione analogico/digitale, la compattezza e leggerezza in peso del design, la scalabilità del sistema, e la praticità intrinseca dello storage su SDcard accoppiata alla totale modificabilità via USB del software contenuto nel datalogger, rendono questo sistema un'interessante alternativa alle soluzioni in commercio.

Vengono presentate le installazioni effettuate nel corso del 2010 in Costa Rica (con l'appoggio del CATIE - Centro Agronómico Tropical de Investigación y Enseñanzaed) ed in un'azienda sperimentale a Pontedera (in collaborazione con la Scuola di Studi Superiori Sant'Anna di Pisa) dei primi datalogger costruiti; sono riportati inoltre i primi dati ottenuti.

Summary

In the trees, water moves through a negative pressure gradient established between roots and leaves, through a network of xylem cells whose length can reach the order of magnitude of 100 meters in the higher plants on the planet.
The grandeur of the transport system involves the need for the plant to implement some tricks to cope with the increasing hydraulic resistance related with the dramatic lengthening of the water path throughout the ontogeny. That is to say that the increase in plant height is accompanied by a consequent increase of the total hydraulic resistance within the xylem conduits. The most effective solution to contain the increase of hydraulic resistance seems to be the tapering of the conduit elements.
The introduction by WBE (West, Brown, Enquist 1997, 1999) model of the hypothesis of universality of the degree of xylem conduit tapering in vascular plants, leads to introduce a threshold value of the "optimal" degree of tapering such that the hydraulic resistance of a path is approximately constant regardless of its length (the conduit is always potentially capable of growing). It was therefore suggested that the nature of hydraulic limitations to growth in plant height may be the result of a sub-optimality of the degree of tapering caused by the physical inability to increase cell diameter at the base indefinitely. Alternatively, it is possible that a sub-optimality of the overall transportation system can occur at some point of the development in height (and therefore in length and volume of xylem conduits) due to the impossibility of maintaining a state of optimum equilibrium of the conduction system, designed as a transport network optimized (Banavar, Maritan, Rinaldo 1999) when the volume of service inside the network and the hydraulic resistance resulting in the displacement of this volume, are both minimized in a logical solution of a minimum equilibrium bound problem.
One of the objectives of this work has been put together two of the main models proposed recently to the attention of the scientific community (the WBE model and the model BMR) and to collect them in the development of a new unique

model, to try to answer the fundamental question implied in this research topic: "which factors causes the plants to stop growing in height?".

In the first part, the work is a short but sufficiently detailed analysis of the assumptions of the WBE model and model BMR, in which are showed the main steps leading to the results contained in both models, and the results.

Within the same chapter is then given space to the model proposed by this thesis, in which it is solved a problem of constrained minimum where a powerlaw shape conduit (adhering to the assumptions of the WBE model and not in contradiction with the hypotheses made for transport network in the BMR model), passes a continuous variation of shape between the two extreme and opposed solutions of the problem: the shape of minimum resistance (a cylinder) and the shape which realize the minimum service volume (a truncated cone), looking for the best compromise solution. The reasons because it is not possible to achieve a closed-form mathematical solution of the problem are analyzed, and it is developed a software algorithm to solve the model. At the end, it is showed the solution proposed by our model, also obtained from the input data of real plants, all converging to a single stable solution of constrained optimization.

The second part of this paper describes an heating experiment of the apeical gem of treeline trees to discuss the importance of tapering in conduit elements of coniferous species (*Pinus cembra, Larix decidua* and *Picea abies*) and in particular to show the importance of temperature in limiting the growth in height.

The experiment described in second chapter and conducted over two growing seasons, has given us a way to think about the ideal characteristics that should be used in field instrumentation and in particular the usefulness of having data acquisition devices that are effective, economical and reliable, if necessary modular and reprogrammable as needed.

In the last part is then presented the project and implementation of a data logging system based on the philosophy of free software. In parallel with the other research activities, the last two years of my PhD have also been used for the construction of a data acquisition system based on the Arduino open source

hardware platform, aimed in particular for the datalogging of Granier-type sensors for sap flow measurement in plants.

The datalogger made offers several advantages over the solutions proposed by the major companies operating in the data acquisition field in science. Regardless of the considerable cost of the system designed in fact, the precision offered in analog / digital conversion, the compactness and light weight design, system scalability, and ease of storage SDcard intrinsically coupled to the total modifiability of the datalogger software via USB makes this system an interesting alternative to the market solutions.

In the same chapter are presented the installations carried out during 2010 in Costa Rica (with the support of CATIE - Centro Agronomic Tropical de Investigación y Enseñanzaed) and in a farm in Pontedera (in collaboration with the School of Advanced Studies Sant'Anna, Pisa, Italy) for which we built the first data logger. Are also reported the first collected data.

Index

1 An integrated model based on WBE and BMR hypothesis

1.1 Introduction

Biological variables in trees, such as in many other biological processes, are characterized by allometric scaling relationships with body mass or size. So that for a generic biological variable *Y*, these relationships follows the typical power-law form:

$$Y = Y_0 M^b$$

where *Y* is the variable, Y_0 is a normalization constant, *M* is the body mass and *b* is the *scaling exponent*.

While in Euclidean geometry, a *D*-dimensional compact object, has a volume *V*, and a body mass *M,* that scale as the *D*-th power of its linear size, in those systems including a fractal-like transportation network, this *D*-scaling, is no longer valid.

The search for a general allometric relationships explanation drove to the 1997 version of the so-called WBE model (West, Brown and Enquist, 1997). In the first version, the results of WBE model could not be applied to plants so in 1999 an "integrated version" of the model was proposed, pointing out the fact that the network counduits must taper (as proposed by Zimmermann, 1978) and in consequence of this, the total hydraulic resistance of the fluid flow among a path is almost independent of the total path length. Many works confirmed then many observations of conduit tapering in trees (Anfodillo et al. 2006; Weitz et al. 2006; Coomes et al. 2007; Petit et al. 2008).

As a general model, WBE has been criticised for being biologically unrealistic and for mathematical inconsistance by many authors (Kozlowski and Konarzewski 2004; Makarieva et al. 2005; Coomes 2006, Petit and Anfodillo 2009), anyway, WBE model has received huge attention from the scientific

community, and stimulated many works about allometric scaling relationships among the so-called “metabolic theory of ecology” line of research.
The point we focused on in our research is that even if a tree can design a xylem network in which total hydraulic resistance is kept almost constant, this is still not enough to let the tree grow up forever, and despite a tree can reach really impressive heigths, there are at the end some factors that drive it to stop growing, and eventually after many years, to hydraulic stress conditions and then to dead.
Since trees have no pulsatile organs for pumping sap flow into xylem conduits, and the functioning of transportation network is just driven by the different pressure potential between roots and leafs, we considered that the network functioning must obey to other requirements more than just the minimum hydraulic resistance principle.
In 1999 the BMR model (Banavar, Maritan, Rinaldo 1999) derived a general allometric relationship between size and flow rates valid for inanimate systems, starting from observations on river drainage basins. BMR model was also criticized for mathematical controversial (Makarieva et. al 2005) in particolar for concluding that the total mass / volume of distributive network grows up faster with the system size than the total mass, while it is imposed that the distributive network is included within the body that it supplies. Anyway the minimum service volume principle seems to be a good constraint for an integrated model, so we combined WBE and BMR hypothesis to try to explain the stop-growing status of trees.

1.2 A brief review of WBE (97&99) and BMR Models

WBE Model provided a first general explanation of the 3/4 power law (Kleiber, 1932) in biology, leading to the following relation between metabolic rate and mass of an organism:

$$B \sim M^{3/4}$$

WBE Model relies on the following assumptions (West et al. 97, West et al. 99):

(1.1) The network a is strictly hierarchical and self similar *space filling* fractal-like branching network (Mandelbrot, 1982).
(1.2) The number of orders of branching is very large.
(1.3) The terminal elements are size-invariant.
(1.4) Diameters among different orders of branching can vary in size. In particular conduit elements must taper along levels.
(1.5) The network minimize the total hydraulic resistance along the path.

With these assumptions, WBE model demonstrates that,

(1.6) If

⇒ the increasing ratio of radius from basal level to the (top) terminal level is:

$$\overline{\beta} = \frac{d_{k+1}}{d_k} = n^{-\bar{a}/2}$$

where d is the conduit raiuds, k is the k-th level of branch, and $\bar{a}$ is the conduit tapering ratio.

(1.7) And

⇒ the counduits conductance, calculated via the Huygen-Poiseuille equation[1] (achieved for laminar flows in capillar tubes), is conserved among levels, so that: $\frac{\pi d_k^4}{8\eta l_k} = \frac{\pi d_{k+1}^4}{8\eta l_{k+1}}$

[1] The assumptions of the Hagen–Poiseuille law are that the flow is laminar, viscous and incompressible and the flow is through a constant circular cross-section that is substantially longer than its diameter. The fluid flow will be turbulent for velocities and pipe diameters above a threshold, leading to larger pressure drops than would be expected according to the Hagen–Poiseuille equation.

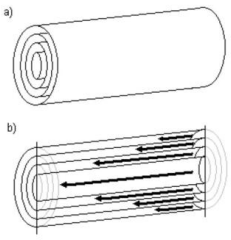

(1.8) And

⇒ the proportionality of branches for *n* branching generations in the *space filling* network is:

$$\gamma = \frac{l_{k+1}}{l_k} = n^{-1/3}$$

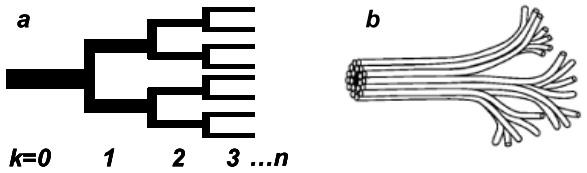

Fig. 1.1 Branching structure from West et al. 1999. **a**. Topology of plant branching network. **b**. Symbolic representation of branch vascular structure, showing conducting tubes and non-conducting tissues (black).

(1.9) Then:

⇒ for $\bar{a} \to 1/6$ the hydraulic resistance (calculated via the Huygen-Poiseuille formula) of total path is constant over length:

$$R_{TOT} = \sum_{k=0}^{N} R_k = \left[\frac{1 - \left[\left(n^{1/3} - 1 \right) \cdot l_{TOT} / l_N \right]^{(1-6\bar{a})}}{1 - n^{(1/3-2\bar{a})}} \right] \cdot R_N \xrightarrow{\bar{a}=1/6} \text{cost.}$$

where:

l_{TOT} = total path length (i.e., tree height)

R_N = hydraulic resistance of the terminal elements.

See fig. 1.2.

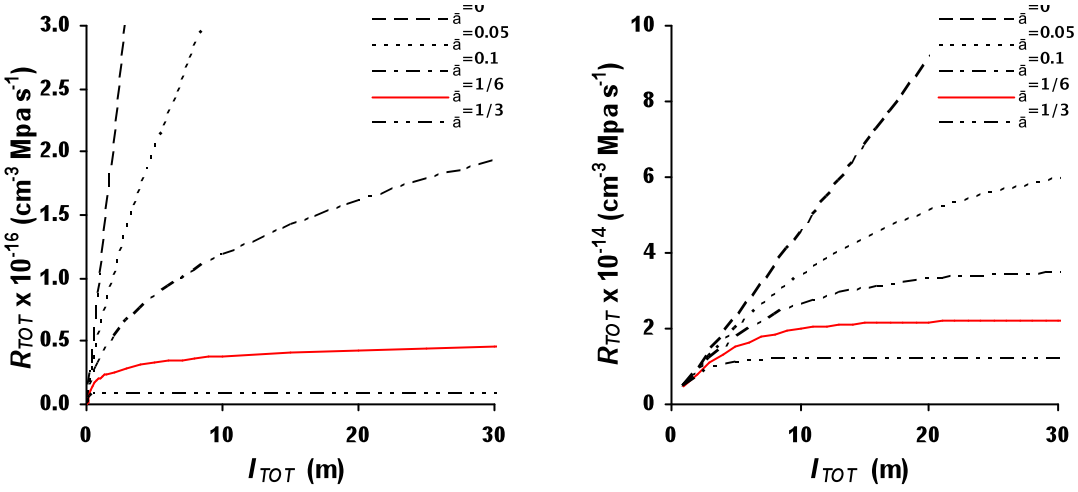

Fig. 1.2 Relationship between total hydraulic resistance (R_{TOT}) and total path length (l_{TOT}) for various degrees of conduit tapering ($\bar{a}$). (Left): length and conduit radius of elements scale with l_{TOT} as stated by the WBE model (West et al. 1999), with l_N=0.05 m and d_N=6 µm. (Right): the length of elements is kept constant (1-m-long) all along the pathway and d_N=6 µm (Becker et al. 2000).

WBE Model has been hardly criticized for mathematical and logical controversial, but had the merit of introducing the concept of conduit tapering as a solution to keep hydraulic resistance almos constant over the grow of trees in height.

In 1999 J. Banavar, A. Maritan, A. Rinaldo, proposed another Model (hereafter BMR model) wich seeks to explain the quarter-power scaling law.

BMR make use of similar basic assumptions of WBE model achieving the result of allometric relationship between the mass *M* of an organism and the metabolic rate *B* (formally “the total amount of nutrients being delivered to the transfer sites per unit time”):

$$B \sim M^{3/4}$$

A considerable point of BMR Model is the definition of the most efficient class of networks as that for wich the total “blood volume” *C* is as small as possible. (This does not coincide with the assumption -made in the WBE model- of a hierarchical network in wich hydraulic resistance is minimized).

The key result of BMR model is that:

(1.10) If

⇒ we consider ANY spanning network in D dimensions

(1.11) And

⇒ the object we are considering (wich contain this network) is characterized by a linear size L

(1.12) And

⇒ the total mass M of the considered organism scales as the total blood volume C

(1.13) And

⇒ the flow transfer at terminal elements is indipendent of organism size

(1.14) And

⇒ the number of transfer sites scales as L^D. Wich also means that the metabolic rate B scales as L^D.

(1.15a) Then:

⇒ in the most efficient class of networks (defined as those in wich the total blood volume C is as small as possible):

$$C \sim L^{(D+1)} \qquad \text{(and for large } L, C \sim L^{2D}\text{)}$$

From this result, we can also obtain the Mass/Metabolism allometric scaling. In fact, if we combine the key result (1.15a):

$$C \sim L^{(D+1)} \Rightarrow \text{(2.15b)}\ L \sim C^{(D+1)^{-1}}$$

with (1.14):

$$B \sim L^D$$

we obtain:

(1.16) $$B \sim C^{\frac{D}{D+1}}$$

Considering now (1.12):

$$M \sim C$$

and combining (1.16b) & (1.12) we get:

(1.17) $$B \sim M^{\frac{D}{D+1}}$$

In the case of D=3, this result leads to:

(1.18) $$B \sim M^{\frac{3}{4}}$$

Despite some disputes between authors and critics to the BMR model (Makarieva et. al 2005, Petit 2007), the "minimum blood" definition of efficient class networks led us to a new point of view in wich we compared WBE and BMR models.

1.3 WBE and BMR integrated model

We considered the optimum criterion of minimum hydraulic resistance insufficient to explain the stop growth of trees so we integrated the WBE optimum condition of minimum resistance with the BMR optimum condition of minimum service volume, creating a minimum problem with two constraints.
The idea is to find the optimal shape that a powerlaw tapered conduit must reach to obey both constraints: *min[Volume].AND.min[Resistance]*.
Of course, those two constraints are opposed. In fact, if we consider a tapered conduit that joins two diameters of our choice (let's say a basal diameter and an apical diameter, with base > apex), then the conduit that has minumum resistance is a cylinder (eventually with a short final shrinkage), and that with minimum volume is a trunk-cone.
Since we wanted to compare many shapes between the two cases (cylinder and trunk-cone), we had to normalize conduit length, and let vary the tapering/shape exponent.

Unfortunately, if we consider a conduit shape (which total length is *L*) in the form:

(1.19) $d = d_{h(N-1)} \cdot l^{b}$

$d_{h(N-1)}$ is apex diameter;

l is the conduit length (going from *0* to the total conduit length *L*);

and we solve a system in which both minimize the following:

(1.20) $min\ [V = \pi \int_0^L r^2 dl\ ]$ Volume

and (1.21) $min\ [R = \frac{\pi}{8\eta} \int_0^L \frac{r^4}{l} dl\ ]$ Resistance (Poiseuille Law)

with: $r = r(l)$

then the problem is indeterminate in a close form.
We developed different models to solve this problem, and while doing this we also chanced some points about the structure of the model, to be able to solve it. The different models can be found in the appendix of this chapter.

The final version of our model can be explained as follow. First of all we must consider a relative total conduit length of "1" to be able to compare different powerlaw shapes with the same initial and final diameters to find that optimum one with *min[Volume].AND.min[Resistance]* by letting vary the powerlaw exponent from $b \to 0$ (a cylinder conduit shape with the *min[Resistance]*) to $b \to 1$ (a truncated cone shape with the *min[Volume]*).

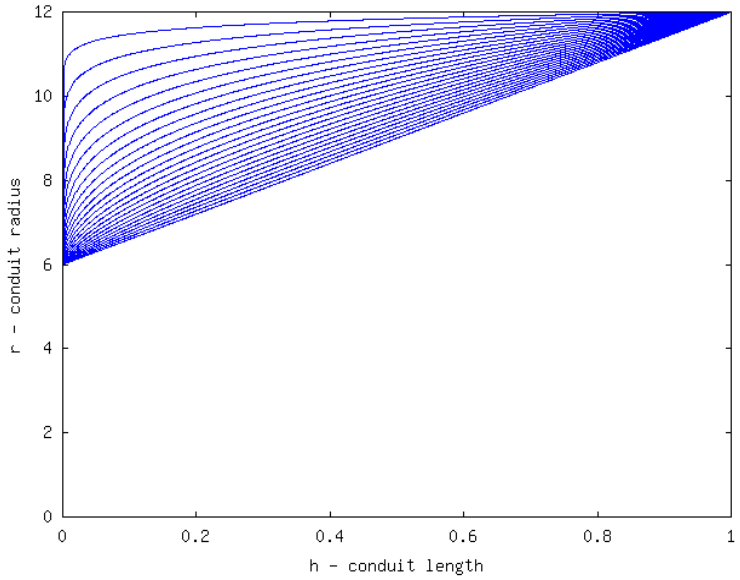

Fig. 1.3 Simulations of a conduit section (half conduit profile is showed) joining a terminal diameter of 12μm with a basal diameter of 24μm. The model devises 10000 steps of the *b* exponent from 0 (cylinder: *min[Resistance]*) to 1 (trunk-cone: *min[Volume]*). Volume and Resistance are calculated by the model for each shape (the figure is an example with less then 10000 steps, to make it visible the carried process).

As a first step in our work, we considered a constant apical diameter (12 μm) and a ratio between apical section and base section, to check the stability of the optimum solution. So we simulated 10000 powerlaw shapes varying the *b* exponent (1.19) from 0 to 1. See Fig. 1.3. The optimum exponent we obtained is about 0,18 and it is compatible with both the WBE predictions and the data collected from trees.

Since we wanted to simulate many different boundary conditions of conduits based on real trees data, we had to be able to use the real tree height, apical and base diameter of those trees being analyzed in our department, as an input for the model.

The necessary trick of considering the relative total height equal to "1" is then binding to let vary the triad "height, apical diameter, base diameter". This had to be solved, so we introduced a proportionality coefficient *"T"* formally and conceptually equivalent to the *"T"* coefficient introduced in Anfodillo et al, 2006.

This coefficient expresses the ratio between the base radius (*rbase* or $d_{h(0)}$; l=1) and apex radius (*rapex* or $d_{h(N-1)}$; l=0) and by doing this it is also representative of the tree height:

$$T = \frac{rbase}{rapex} \quad (1.22)$$

By varying the T coefficient from 1 to 4 (T < 1 would mean unrealistic reverse tapering) it is as if we consider trees in wich the conditions of maximum growth are far (T small) or close (T high) because the base diameter can still be increased or not.

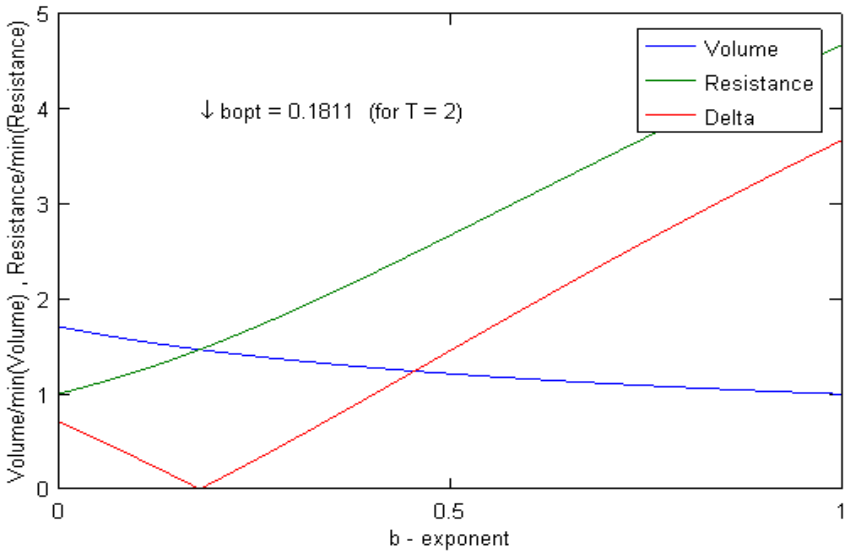

Fig. 1.4 Example of the output graph from the model. Different colors represents Volume, Resistance and their Delta, for one instance of the minimum problem. So for T=2, the optimum result achieved by the model is a power-law tapered conduit which exponent is b=0.1811.

For each T chosen between 1 and 4, the minimum problem has been solved to find out the best exponent b (see Fig. 1.4). This variation of T was also useful to check the stability of the solution among different boundary conditions. See Fig. 1.5.

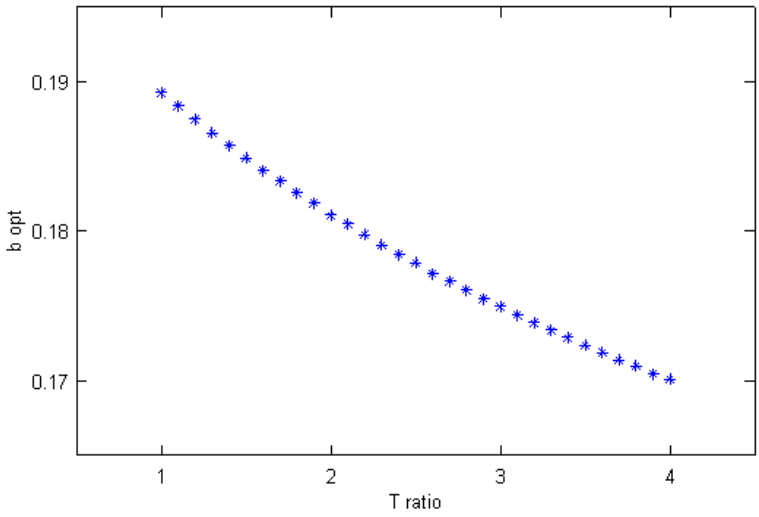

Fig. 1.5 To check the stability we did change the coefficient *T* from 1 to 4 with steps of 0.1, and solved for each condition the minimum problem. In real trees this coefficient is usually between 1,5 and 3. We can see that the solution is stable.

In the final model we used two input data extrapolated from each tree at our disposal: the apical diameter and the *T* coefficient.

The result for each different input combination ($d_{h(N-1)}$,*T*) is in the range of *b*=0,175..0,187. See Tab. 2.1 and Fig. 1.6.

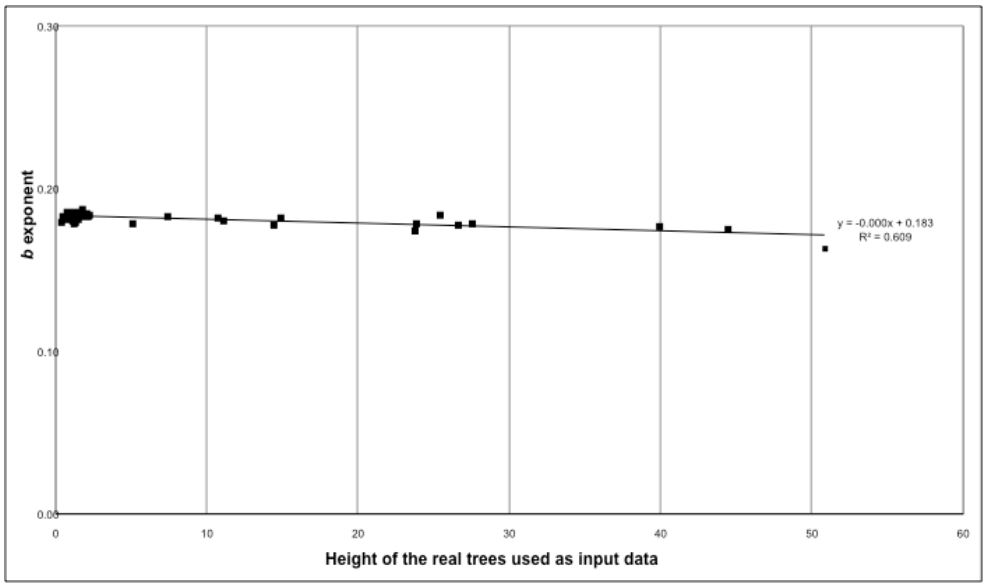

Fig. 1.6 Results of the *b* exponent for different input data collected from trees. The trend result is *b=0,183*.

Tree	Height l (m)	D h0 (micron)	D hN-1 (micron)	T coefficient	Cells Profile Slope	Model solution *b exponent*
FE15	14,400	103,800	43,620	2,380	0,300	0,1780
LD27	26,600	47,850	19,300	2,479	0,169	0,1780
LD40	39,900	43,960	16,260	2,704	0,177	0,1770
PA44	44,400	43,270	14,270	3,032	0,196	0,1750
GS14_2004	11,080	50,245	24,417	2,058	0,193	0,1807
GS17	14,900	45,914	24,486	1,875	0,205	0,1820
S18	5,121	53,451	23,034	2,320	0,168	0,1790
GS47	10,700	41,499	22,651	1,832	0,168	0,1824
GS110	7,430	47,519	26,247	1,810	0,203	0,1825
S15	27,550	52,545	22,444	2,341	0,182	0,1789
Picea_rob*	25,380	41,091	25,598	1,605	0,195	0,1841
GS498	1,310	47,336	21,252	2,227	0,236	0,1796
GS497	1,765	47,257	38,473	1,228	0,062	0,1872
S16	2,120	48,199	27,770	1,736	0,153	0,1831
S47	23,750	76,595	24,794	3,089	0,129	0,1745
GS14_1	1,108	50,245	24,417	2,058	0,193	0,1807
GS14_2	2,245	49,940	29,489	1,694	0,154	0,1834
GS18	0,785	43,886	22,479	1,952	0,159	0,1815
SG499	1,120	43,544	25,355	1,717	0,144	0,1832
Pc-C22	0,800	21,357	15,248	1,401	0,157	0,1857
Pc-C2	1,570	26,690	16,276	1,640	0,258	0,1838
Ld2	0,810	26,132	16,326	1,601	0,178	0,1841
Ld4	1,280	30,536	20,814	1,467	0,166	0,1852
Ld5	1,660	30,019	19,321	1,554	0,208	0,1845
PS16_2005	2,070	24,909	16,420	1,517	0,103	0,1848
PS19_2005	1,060	24,604	16,601	1,482	0,101	0,1851
PS20_2005	1,260	23,387	16,199	1,444	0,107	0,1854
PS20_2006	1,459	24,194	14,000	1,728	0,142	0,1831
MR_4F_2007	0,748	23,590	13,848	1,703	0,159	0,1833
MR_4F_2005	0,618	22,912	12,895	1,777	0,186	0,1828
MR_5F_2007	0,490	17,718	9,289	1,907	0,198	0,1818
MR_5F_2005	0,385	20,846	9,475	2,200	0,269	0,1798
MR_1R_2005	1,040	22,149	12,198	1,816	0,158	0,1825
MR_3R_2005	1,035	21,123	12,286	1,719	0,160	0,1832
MR_4R_2005	1,180	25,507	11,635	2,192	0,202	0,1789
SV_1F_2007	1,469	22,644	11,453	1,977	0,166	0,1813
SV_2F_2007	0,790	18,175	11,979	1,517	0,128	0,1848
SV_3F_2007	1,870	21,701	12,230	1,774	0,150	0,1828
SV_3F_2005	1,490	21,598	12,828	1,684	0,124	0,1835
SV_4F_2007	1,490	21,763	12,571	1,731	0,150	0,1831
SV_5F_2007	0,438	24,879	14,124	1,761	0,207	0,1829
SV_3R_2005	1,520	21,370	12,850	1,663	0,130	0,1836

Tab. 1.1 Input data and model result (*b exponent)*.

1.5 Discussion

We believe that the hypotheses formulated in the WBE and the BMR models are consistent. In particular, with this work we suggest that the optimality criterion of a transportation network which conduits are independent, tapered and based on both the conditions of minimum service volume and minimum hydraulic resistance, leads to the establishment of a conduit tapering solution that expresses the conditions of maximum growth potential of a tree.

The "optimum" degree of tapering achieved by our model, would therefore be representative of the "steady state" that can persist when a tree has reached its growth potential, namely when the xylem conduits are shaped in such a way that any modification of their shape in order to grow further would fall out of the tapering exponent we just assumed. The value of 0.18 for the tapering exponent would therefore be descriptive of an ideal condition to which trees tend in their growth, having xylem conduits whose degree of tapering is located now below, now above this value due to environment / real-life conditions, in the various stages of existence of the tree outside the ideal conditions.

1.6 Chapter appendix: Model algorithms

1.6.1 First model

The model could calculate Volume and Resistance for a powerlaw shaped predetermined conduit.

Language: Fortran.

```
1          Program ModelTree
2
3          implicit none
4          integer i
5          double precision a, b, deltah, ri, voli, voltot
6          double precision resi, restot, resmax
7
8    *     INPUT
9          OPEN (1, FILE = 'risultati.csv')
10         a=13
11         b=0.001
12            write(6,*)'|     |      |       |            |            |'
13            write(6,*)'|  H  |  b   |  Ri   |   ResTOT   |   VolTOT   |'
14            write(6,*)'|     |      |       |            |            |'
15   *                 3000   0.001  25.434  0.32275E+13  0.60816E+11
16   100   restot=0
17         voltot=0
18         i=1
19         deltah=1000  !  deltah = lungh cell, in micron
20         resmax=4E+012
21
22   20    FORMAT(2x,I4,2x,F5.3,2x,F9.4,2x,E11.5,2x,E11.5)
23   30    FORMAT(I4,',',F5.3,',',F9.4,',',E11.5,',',E11.5)
24
25   200   ri=a*(i*deltah)**b
26   *     calcolo res. idraulica con Poiseuille
27   *     resi=((128*0.0011/3.14159265358979)/((ri/10000)**4))
28         resi=((8*0.0011/3.14159265358979)/((ri/10000)**4))
29         restot=resi+restot
30         voli=deltah*3.14*(ri**2)
31   *     voli=2*3.14*ri*deltah  ! Caso con "Volume di spesa" / Carbonio
```

```
32          voltot=voltot+voli
33  *       IF (restot < resmax) then
34  *       write(6,*)i, ri, restot, voltot   ! stampa a video di controllo
35          i=i+1
36          IF (i<=3000) THEN
37           GOTO 200
38          endif
39          write(6,20)i-1, b, ri, restot, voltot
40          write(1,30)i-1, b, ri, restot, voltot
41
42          IF ((b<=1.4) .AND. (ri<200)) THEN
43          b=b+0.001  ! incremento
44          GOTO 100
45          endif
46
47          write(6,*)'Programma Terminato - File csv scritto.'
48          stop
49          end
```

1.6.2 Final model

The model receives input data of apical diameter $d_{h(N-1)}$ and coefficient T. The output is exponent b of the optimum powerlaw conduit for minimizing Volume and Resistance. (the output is provided also as a graph showing volume and resistance, see Fig. 1.6).

Language: Matlab/Octave.

```
clear;
treename={'Tree Cembro','Tree Larice','Tree Picea','Tree Eucalipto_1'};
alldapex=[15.481 14.507 25.598 51.641];
allT=[2,161 3.116 1.605 3.477];
for numinput=1:length(allT)
      dapex=alldapex(numinput);
      T=allT(numinput);
      bstart=0;
      bend=1;
      bsinc=0.01;    % FAST=0.01 - COMPLETE=0.0001
      bvect=[bstart:bsinc:bend];
      rapex=dapex/2;
      htot=1;
      steps=10;      % FAST=10 - COMPLETE=1000
      sinc=htot/steps;
      h=[0:sinc:htot];
      for f=1:((bend/bsinc)+1)
            b=bvect(f);
            r=rapex*(1+(T/2)*h.^b);
            vol(f)=0;
                res(f)=0;
            for i = 2:(steps+1)
      vol(f)=vol(f)+pi*((((r(i)+r(i-1))/2)^2)*sinc);
      res(f)=res(f)+((sinc*8*1.11*(10^(-7)))/(((((r(i)+r(i-
                                                  1))/2)/10000)^4)*pi));
            endfor
      endfor
      for f=2:((bend/bsinc)+1)
            if(abs(res(f-1)/min(res)-vol(f-
```

```
                    1)/min(vol)))>(abs(res(f)/min(res)-vol(f)/min(vol)))
29                  bmin=bvect(f);
30              endif
31        endfor
32        bopt=bmin;
33        figure(numinput);
34          set(0,'defaulttextfontname','*')
35        plot(bvect,vol/min(vol),";Volume;",bvect,res/min(res),";Resistance;");
36        axis([0 1 0 10]);
37          set(gca,'XTick',[0:0.1:1]);
38          set(gca,'YTick',[0:0.5:10]);
          text(bmin,7, strcat('\downarrow bopt = ',num2str(bopt),'  ( T = ',
39                              num2str(T),' & Dapex = ',num2str(dapex),')'));
40        text(bmin,7.7,treename(numinput));
41        xlabel('b - exponent');
42        ylabel('Volume/min(Volume) , Resistance/min(Resistance)');
43        switch (numinput)
44              case 1
45              print -deps Tree Cembro.eps;
46                  case 2
47              print -deps Tree Larice.eps;
48                  case 3
49              print -deps Tree Picea.eps;
50                  case 4
51              print -deps Tree Eucalipto_1.eps;
52        endswitch
53  endfor
```

2 Heating experiment on treeline plants

2.1 Introduction

To study the importance of the apical diameter on the entire xylem growth, we conducted an experiment (Petit et al. 2010) in changing microclimatic conditions of the apical stem during the growing season 2006 and 2007 to some selected plants at different altitudes.

At high altitude (treeline), the physiology of trees is hardly hampered by the extreme environmental conditions: low temperatures are generally responsible for the delayed cambial reactivation (Gričar et al. 2006; Rossi et al. 2007; Riondato 2009) and an overall reduction in the duration of the growing season can be observed. In fact, the length of time needed for cell division and expansion seemed to increase with decreasing temperatures, approaching infinity at +1 to +2 °C.

The study area was located in two different sites in the Dolomites (Easter Alps, Italy) to have different altitude/temperature conditions.

A first study site was setted up at High Altitude (hereafter: HA) at Monte Rite (2100 m asl, Cibiaba di Cadore, BL, Italy) where the treeline is mostly composed by *Picea abies* Karst and *Larix decidua* Miller plants. The other site was located at Low Altitude (hereafter: LA) nearby the Research Center for Alpine Ecology of the University of Padova (1100 m asl, San Vito Di Cadore, BL, Italy), in a typical mountain forest, mainly composed by *Picea abies, Larix decidua and* other secondary species. The specie selected for this study was *Picea abies* Karst.

2.2 Materials and methods

In both HA and LA sites an heating system was applied to the apical stem of five plants (H1 to H5), and a similar non-heating system was applied to other five similar growing plants as control (plants C1 to C5).

To set up a proper heating device, ten polycarbonate cylinders (length 250 mm; diameter 50 mm; thickness 3 mm) were coiled each by 20 spires of resistive wire (Omega Engineering, Inc. - USA) creating an 'heating device' that was installed to the apical developing bud of each heated tree, surrounding it (see photos) and so creating a microclimatic chamber where the temperature was mantained always higher than that of the environment, by a constant (+5±0.5 °C at the HA site, and +10±0.5 °C at the LA site).

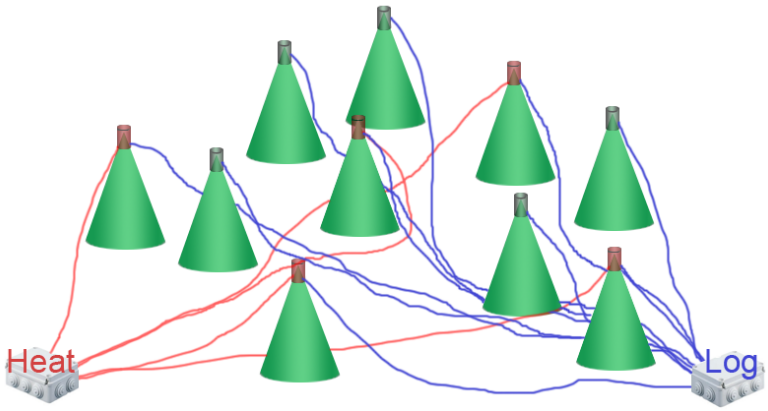

Fig. 2.1 Representation of each study site with heated and control plants. In red the heating system, in blue the loggin system (this is an idealized representation).

Ten other polycarbonate cyilnders (length 250 mm; diameter 50 mm; thickness 3 mm) where not coiled with resitive wire, and were attached to the control trees of each site to simulate the same possible glass-house conditions of the heated ones. See Fig. 3.1.

A temperature probe (made of two thin copper and constantane -type T- wires) was placed inside each cylinder and then connected to a CR10X datalogger (Campbell Scientific Inc. - USA) to log the temperature data for instant and later control.

Another temperature probe was placed outside the cylinder, to record the environmental conditions. The instant data collected from the temperature probes placed inside and outside polycarbonate cylinders are also used by the datalogger to check the difference between the temperature inside and outside the cylinder and to switch on and off an heating circuit when this difference became greater then the chosen tolerance.

The heating circuit is used to keep a constant temperature gap between the apical stem and the environment. The circuit is powered by a regulated power supply unit (30V, 10A, 35W max) and it is very simple: when it is needed, the CR10X logger turns on an electromagnetic relay switch that closes the circuit between the 35W power supply unit and the resistive wire coils. Then, when the inside/outside temperature gap of the cylinder is above the tolerance, the datalogger simply stops powering the raley switch and so the power supply to the heating wire is stopped.
A Wavecom(c) GSM modem (Campbell Scientific Inc. - USA) interfaced to the CR10X datalogger made it possible to query the datalogger and download data from its memory to a remote control room.

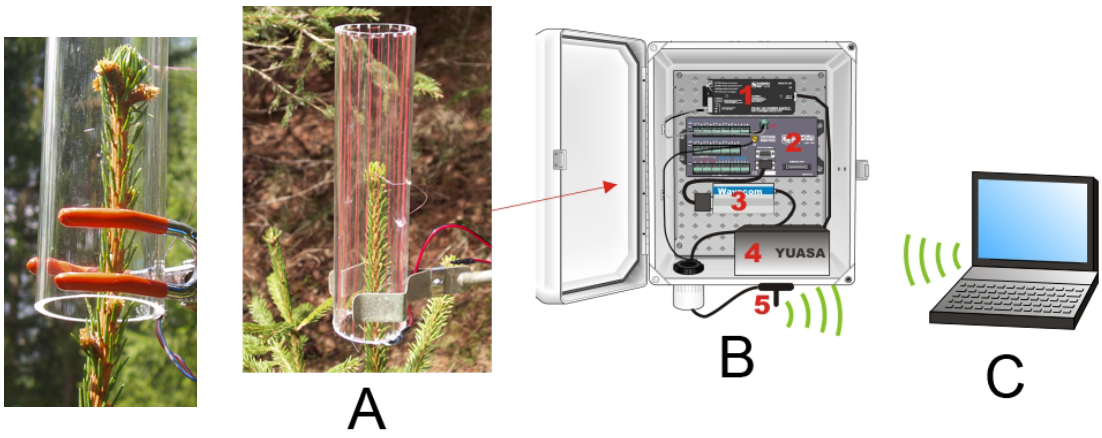

Fig. 2.2
Left: Polycarbonate cylinder (without heating coils) with a temperature probe inside, placed on the apical stem of a control plant to simulate a similar glass-house effect as in the heated plants.
Right: A: Polycarbonate cylinder with resistive heating wire coils placed on the apical stem of an heated plant. B: Circuits enclosure, containing: 1) Power supply unit, 2) CR10X datalogger, 3) GSM Wavecom(c) modem , 4) Heating circuit (electromagnetic switch connected to the resistive wire), 5) Modem antenna. C: Remote pc with the Campbell Scientific's LoggerNet(c) remote datalogger control software.
In both Left and Right installations temperature probes are placed inside and outside the cylinder.

The heating experiment was carried out for two succeeding years to achieve a better evaluation of its effects on tree growth, wich is know to be strongly related to the environment conditions of the previous year in coniferous species (Jalkanen & Tuovinen, 2001).

The heat was supplied from May 19th to July 12th in 2006 and from May 10th to August 16th in 2007 in the HA (Monte Rite) site; from April 28th to September 13th of 2006 and from April 19th to August 21th in 2007 at the LA (San Vito) site. At the beginning of September 2007 all trees were felled to make the proper cell measurements.

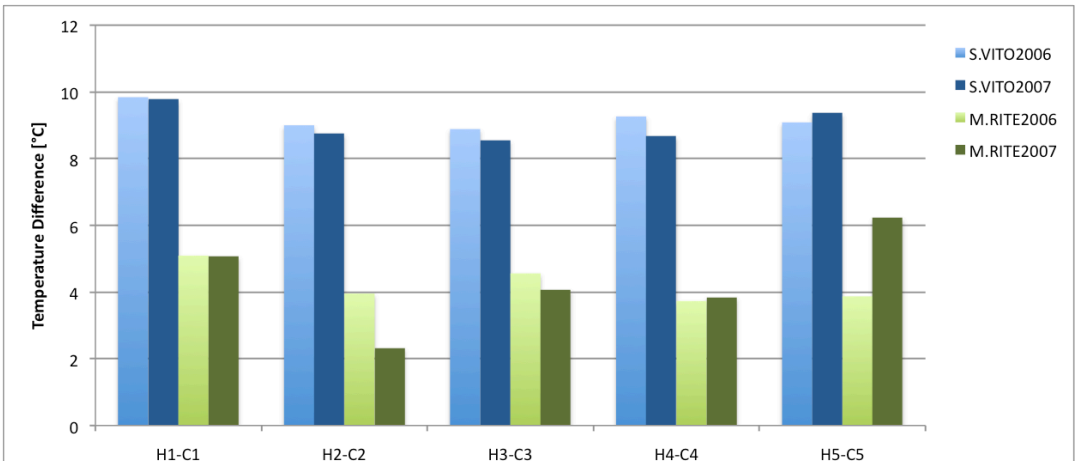

Fig. 2.3 Average difference of temperature between Heated and Control trees, in the two study sites (M.RITE-HA and S.VITO-LA), over years 2006 and 2007.

2.3 Anatomical analyses

For each tree, the total height, basal diameter and stem annual longitudinal increments were measured. Along the stem, wooden disks were carefully extracted at 2 cm for the distal node of the last four internodes. Other 6-8 disks were extracted lower down at different distances along the stem. For each sampling point, the stem diameter and relative distance from the apex were measured.

Wooden disks (or at least two/three opposite portions of them comprising zones with no reaction wood, injuries or scars) were embedded in paraffin (Anderson & Bancroft 2002); transverse sections of 10-12 µm were then cut with a rotatory microtome, stained with safranine (1% in water) and fixed permanently on

microscope slides with Eukitt (BiOptica, Milan, Italy). Digital images of the sections were taken at 100x magnification using a light microscope (Nikon Eclipse80i). Lumen areas were measured by WinCell software (Régent Instruments Inc., Sainte-Foy, QC, Canada). Conduits were considered to be circular and, in order to eliminate their endings, only those with a lumen diameter greater than half the diameter of the largest conduit (James et al. 2003) were chosen to estimate the hydraulically weighted diameter, *Dh*, of the annual rings relative to 2005 and 2007:

$$Dh = \frac{\sum d_n^5}{\sum d_n^4} \qquad \text{equation 2.1}$$

where d_n is the n^{th} conduit diameter (Sperry et al. 1994; Sperry et al. 2005).

2.4 Statistical analyses

The scaling parameters of the allometric equations were determined from pairwise comparisons of $\log_{10}$-transformed data. Using reduced major axis (RMA) analysis, the scaling exponents and allometric constants were identified as the regression slopes (αRMA) and *y*-intercept (βRMA), respectively. Regression coefficients, their 95% confidence and prediction intervals, were computed by standard methods (Sokal & Rohlf 1981) using a bootstrap procedure with 100,000 replications (Davison & Hinkley 1997).
Analyses of non linear regression and of variance were performed using *SAS 8.02* (SAS Institute, Cary, N.C., USA).

2.5 Results

The development of the current apical shoot was well described by a logistic function (Fig. 2.4 and Tab. 2.1 – Tab. 2.2). The parameter *c*, which is a coefficient specifying the shape of the curve, i.e., the steepness of the line

between the two inflection points, was considered as an index of the developmental speed of the terminal shoot. It resulted as significantly higher in heated trees at San Vito (t=3.58, p=0.007 in 2006; t=2.82, p=0.042 in 2007), whereas statistics did not reveal any difference between treatments at Monte Rite (t=1.86, p=0.099 in 2006; t=2.32, p=0.075 in 2007).

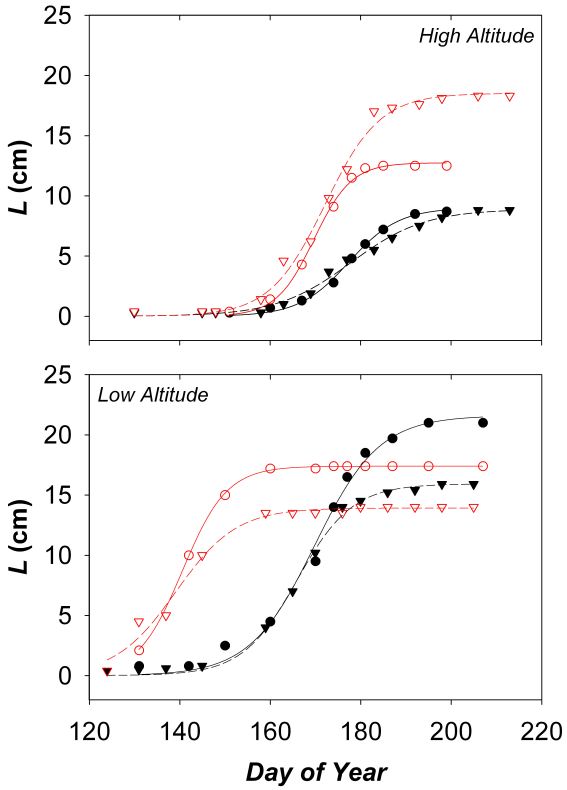

Fig. 2.4 Development of current apical shoot during the growing season in control (solid symbols) and heated trees (empty symbols) during 2006 (circles) and 2007 (triangles). Examples are given of the stem elongation of tree 3C and of 3H at HA (above) and of 4C and 4H at LA (below).

MONTE RITE 2006						
ID	***r^2***	***F***	***p***	***a***	***b***	***c***
1C	0.995	1231	<0.0001	14.99	4.51	0.17
2C	0.971	236.61	<0.0001	6.58	4.01	0.15
3C	0.999	1610.54	<0.0001	9.01	4.97	0.18
4C	0.988	624.12	<0.0001	7.86	4.76	0.20
5C	0.975	278.78	<0.0001	4.91	4.66	0.18
1H	0.990	733.82	<0.0001	16.10	4.48	0.19
2H	0.989	679.88	<0.0001	10.63	5.35	0.24
3H	0.997	3232.54	<0.0001	12.74	4.74	0.24
4H	0.977	368.69	<0.0001	5.61	4.34	0.20
5H	0.980	609.65	<0.0001	4.24	2.60	0.17
SAN VITO 2006						
ID	***r^2***	***F***	***p***	***a***	***b***	***c***
1C	0.991	1892.48	<0.0001	22.99	2.44	0.11
2C	0.976	524.42	<0.0001	14.01	3.46	0.12
3C	0.989	1157.12	<0.0001	27.30	3.30	0.11
4C	0.992	1089.12	<0.0001	21.59	5.57	0.14
5C	0.998	4449.44	<0.0001	40.14	4.53	0.12
1H	0.999	55446.60	<0.0001	27.06	2.42	0.26
2H	1.000	1285681.00	<0.0001	13.01	1.79	0.36
3H	0.999	24716.80	<0.0001	18.85	3.05	0.27
4H	1.000	97978.10	<0.0001	17.39	2.15	0.20
5H	0.996	5414.52	<0.0001	20.20	2.48	0.15
MONTE RITE 2007						
ID	***r^2***	***F***	***p***	***a***	***b***	***c***
1C	0.976	472.13	<0.0001	11.07	5.02	0.12
2C	0.990	885.00	<0.0001	5.78	6.17	0.13
3C	0.992	1209.69	<0.0001	8.88	5.96	0.12
4C	0.980	596.19	<0.0001	7.17	4.61	0.10
5C	0.993	1642.72	<0.0001	4.47	5.95	0.13
1H	0.993	1657.94	<0.0001	24.89	7.10	0.17
2H	0.999	11132.10	<0.0001	6.90	5.65	0.17
3H	0.995	1925.04	<0.0001	18.49	7.10	0.16
4H	0.994	1903.55	<0.0001	17.27	5.05	0.12
5H	0.998	7557.23	<0.0001	8.41	7.80	0.26
SAN VITO 2007						
ID	***r^2***	***F***	***p***	***a***	***b***	***c***
1C	0.989	1273.74	<0.0001	6.18	4.28	0.15
2C	0.987	1224.36	<0.0001	11.32	3.38	0.14
3C	0.994	1836.24	<0.0001	10.73	5.14	0.12
4C	0.997	3638.10	<0.0001	15.91	7.06	0.16
5C	0.995	2205.23	<0.0001	24.11	5.79	0.14
1H	0.999	29424.80	<0.0001	26.96	3.28	0.26
2H	0.992	5867.47	<0.0001	3.51	3.47	0.17
3H	0.999	24984.20	<0.0001	12.77	4.39	0.26
4H	0.986	1679.90	<0.0001	13.91	2.42	0.15
5H	0.998	9834.14	<0.0001	20.36	5.87	0.30

Tab. 2.1 Variation in current apical shoot length (*L*) with time (days from the first measurement) in 2006 and 2007 at both sites, Monte Rite and San Vito. Estimates for the parameters of the fitting logistic equation: *a* is the upper asymptote (i.e., apical shoot length); *b* is the translation coefficient along the *x*-axis; *c* is the shape coefficient describing the steepness of the curve between the two inflection points.

The current longitudinal increment (i.e., the length of the apical shoot after the second year of heat treatment, 2007), compared to the averaged increment of the 5 years before the treatment (2001-2005), was significantly higher in heated trees at Monte Rite (Paired t-test: t=3.56, p=0.024), while control trees did not present any significant changes in the current shoot length (Paired t-test: t=1.80, p=0.146), nor did trees at San Vito, either the heated ones (Paired t-test: t=1.38, p=0.239) or those provided with unheated cylinders (Paired t-test: t=1.07, p=0.346) (Fig. 2.5).

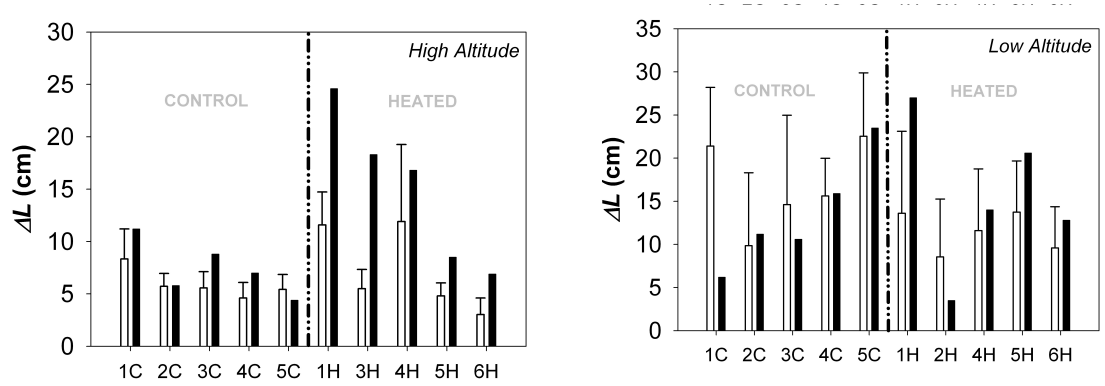

Fig. 2.5 Mean longitudinal annual increment (*ΔL*) over the period 2001-2005 (white; error bars are the standard deviations) and the annual increment of 2007 (grey) of all trees of both sites, Monte Rite (left) and San Vito (right).

At Monte Rite, the apical conduits (at 2 cm from the apex) of heated trees were significantly wider in 2007 (i.e., after the two-years treatment) than 2005 (Paired t-test[2]: t=6.88, p=0.006), while controls did not show any significant difference (Paired t-test: t=0.26, p=0.808). At San Vito, instead, heated trees had similar apical conduits in both 2005 and 2007 (Paired t-test: t=0.51, p=0.637), whereas controls showed a significant reduction in width of lumina of apical cells in 2007 (Paired t-test: t=3.78, p=0.019) (Fig. 2.6).

[2] This paired t-test was performed only on four trees out of five, because the most distal part of the apical shoot of 1H at Monte Rite had burnt after its accidental and prolonged contact with the heated internal resistance of the cylinder.

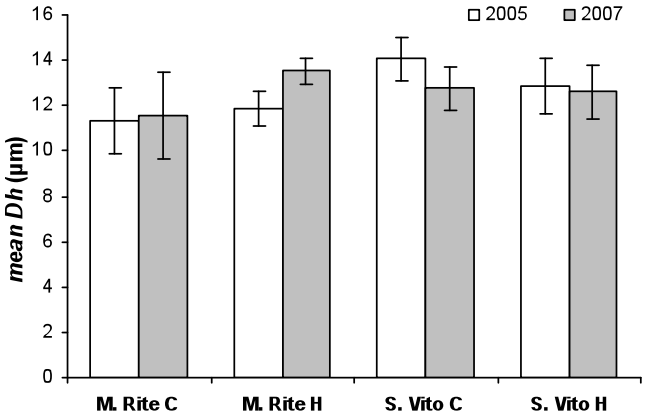

Fig. 2.6 Values of hydraulically weighted diameters (Dh) of the apices of 2005 (white) and 2007 (grey) averaged for treatment (cold, C, and heated, H) and site (M. Rite, high altitude, and S. Vito, low altitude). Error bars represent standard deviations.

In eight trees out of the ten at Monte Rite, the anatomical analyses revealed that the variation in *Dh* with the distance from the apex (*L*) is well described by a power function, with *L* explaining 80-95% of the total *Dh* variance (Tab. 2.2). The $\log_{10}$-transformed scaling coefficient *a* varied from 0.965 to 1.072, while the scaling exponent *b* varied from 0.132 to 0.202 and was significantly smaller than the WBE predicted value of 0.198 in four cases out of the 10 analyzed. Of these four, two concerned the same control tree (i.e., the *Dh* profiles of 1C relative to both 2005 and 2007), whereas the other two cases were relative to *Dh* profiles of 2005 of heated trees. However, this result is certainly affected by the less significance of the power function in 2007 than 2005.

ID	Year	r^2	a	95% CI *a*		b	95% CI *b*		ā	95% CI *ā*	
				min	max		min	max		min	max
1C	2005	0.87	1.07	1.04	1.22	0.15	0.05	0.17	0.12	0.05	0.15
1C	2007	0.86	1.06	1.03	1.11	0.14	0.12	0.17	0.12	0.10	0.14
1H	2005	0.91	1.07	1.04	1.19	0.16	0.08	0.19	0.13	0.07	0.16
1H	2007	0.80	1.01	0.93	1.13	0.16	0.10	0.21	0.14	0.08	0.18
3C	2005	0.91	1.00	0.89	1.05	0.18	0.15	0.27	0.15	0.13	0.22
3C	2007	0.87	0.96	0.76	1.01	0.18	0.15	0.31	0.15	0.13	0.26
3H	2005	0.95	1.04	1.00	1.12	0.16	0.11	0.19	0.13	0.09	0.16
3H	2007	0.87	1.06	0.93	1.10	0.14	0.11	0.21	0.11	0.09	0.18
4C	2005	0.95	1.02	0.93	1.06	0.19	0.16	0.24	0.16	0.13	0.20
4C	2007	0.91	1.05	0.95	1.09	0.16	0.13	0.22	0.13	0.11	0.18
4H	2005	0.98	0.99	0.95	1.03	0.20	0.18	0.23	0.17	0.15	0.19
4H	2007	0.89	1.04	0.92	1.08	0.13	0.11	0.20	0.11	0.09	0.17

Tab. 2.2 Variation of hydraulically weighted diameter (*Dh*) with path length (*L*): estimates for the $\log_{10}$-transformed scaling parameters *a* and *b*, the WBE parameter *ā* and their 95% confidence intervals.

Moreover, we found that the *Dh* at the apex is strictly correlated with the degree of conduit tapering (Fig. 2.7). In our heated trees, in four cases we verified an increase in the dimension of apical conduits coupled with a simultaneous reduction in the degree of conduit tapering. Instead, in H1 we estimated a decrease in *Dh* at the apex accompanied by an increase in *b*, but the actual measurements of lumen areas of conduit at the apex were not possible as the most distal part of the apical shoot had burnt against the internal resistance.

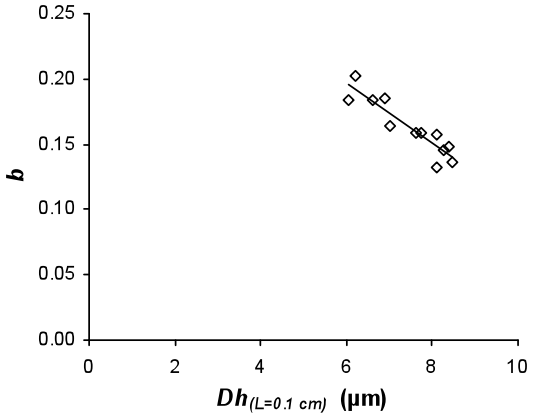

Fig. 2.7 Relation between the hydraulically weighted diameter (*Dh*) at the apex (estimated for each plant from the equation $Dh=aL^b$, with *L*=0.1 cm) and the scaling exponent *b*, describing the tapering of xylem conduits. The equation of the fitting curve (RMA regression) is $b=0.347-0.025 \cdot Dh_{(L=0.1\ cm)}$; $r^2=0.842$..

2.6 Discussion

Our experiment was designed to modify the thermal conditions of the most apical shoots leaving all other parts unchanged. This has enabled us to test the effect of localized heating on longitudinal growth and the importance of thermal environment in determining tree growth at high altitude.

Results appeared to be consistent with the hypothesis that the hydraulic efficiency of the xylem architecture represents a relevant limiting factor for height growth at high altitude.

Overall, our observations confirmed that xylogenesis in trees living in cold environments is significantly stimulated by warmer temperatures (Gorsuch & Oberbauer, 2002; Danby & Hik, 2007). The increase in number and size of conduits enhanced the xylem conductivity. A consequence of the observed tapered profile of conduit dimension along the stem is that the narrower conduits of the apical shoot represent a constraining bottleneck for the whole tree conductance (Becker *et al.*, 2000; Petit *et al.*, 2008). Artificial heating therefore substantially promoted the widening of this bottleneck by increasing both number and size of apical conduits. This triggers a greater hydraulic efficiency of the whole transport system and higher rates of longitudinal growth.

At HA, heated trees grew significantly taller than controls, whereas those at LA showed no significant differences in the newly produced apical shoot length between the two treatments. This is consistent with the observation that the annual increment of leading shoots is particularly affected by low temperatures and therefore leading shoots are generally much shorter in the uppermost trees compared to those growing at lower elevation (Hoch & Körner, 2005).

At LA, the most evident effect of the thermal manipulation on macro-morphology and phenology was the anticipation of bud burst, which was consistent with previous observations (Roberntz, 1999).

The most relevant result of this study was that, after two years, without manipulating any environmental factor other than temperature, heated trees from HA increased stem elongation at rates significantly similar to control trees from LA. This means that temperature alone so far represents the most limiting factor for height growth at high altitudes. Moreover, this effect was obtained by altering the thermal regimes only around the stem apex, which can therefore considered as the thermal “sensor” of the whole tree.

Results of anatomical analyses revealed that the artificial warming promoted hydraulically effective modification only in the newly produced shoots, whereas the remaining xylem tissue (stem) seemed not to show significant changes between pre- and post-treatment.

The analyses of the vertical profiles of conduit diameter revealed that the xylem transport system is organized according to a tapered architecture. Conduits

increased continuously from the stem apex to the base according to a power function, as frequently observed in trees of different species and size (Anfodillo *et al.*, 2006; Weitz *et al.*, 2006; Coomes *et al.*, 2007; Mencuccini *et al.*, 2007; Petit *et al.*, 2008; Petit, Anfodillo & De Zan, 2009). Overall, at HA we observed narrower conduits coupled with higher degrees of tapering (scaling parameter *b*) compared to LA. Tapering results appeared to be in contrast with previous reports of higher rates of conduit tapering in trees at high altitudes (Coomes *et al.*, 2007; Petit *et al.*, 2009).

The lower degrees of tapering observed in trees at low elevation should reflect a minor compensation effect for the path-length resistance with height growth (Becker *et al.*, 2000). Unless conduit tapering was demonstrated to be the most effective mechanism of compensation for the increased resistance with the contextual growth in height (Petit *et al.*, 2008; Petit *et al*., 2010), other important mechanisms of compensation for the increase in path length resistance ought to have been adopted by trees from LA in order to prevent stronger constraint to the water supply to the leaves and consequently to the transpiration and photosynthetic assimilation of atmospheric CO_2.

Comparisons of vertical profiles of conduit diameters pre- and post-warming (2005 vs. 2007) revealed that the effect of heat on xylem anatomy was localized in the last annual shoot.

We therefore hypothesize that the xylem transport system in trees at HA were optimized for water transport according to the higher hydraulic efficiency compatible with the temperature regimes of that environment. Removing most of the hydraulic constraints (Yang & Tyree, 1993; Becker *et al.*, 2000; Petit *et al.*, 2008) by stimulating xylogenesis at the stem apex with artificial warming, we obtained similar height growth to control trees at LA. Instead, increased temperatures did not stimulate height growth at LA likely because those trees are also very sensitive to other kinds of constraints, such as shading or competition with neighbours for resources, or because the applied warming led to supraoptimal temperatures for photosynthetic responses.

Modifications of apical xylem anatomy and their effect on hydraulics and shoot length were more evident after the second year of exposure to increased

temperature, suggesting that anatomical adaptations to changing environment occur gradually over a period of years rather than abruptly from one year to the next.

The importance of this study is that we provided evidence that trees at the treeline undergo temperature-related hydraulic limitations to height growth because of the low efficiency of the transport system due to narrow conduits. We demonstrated that localized warming to the apical shoots promoted a higher carbon investment in xylem conduits (i.e., increased number and/or size). Anatomical modifications occurred only around the heated zones and not along the rest of the stem. This would suggest that the artificial warming, although applied around leaves, did not produce an increase in photosynthetic assimilation of atmospheric CO_2, as supposed by the *carbon limitation hypothesis*. Rather, this would support the hypothesis that low temperatures hamper the fixation of NSCs into biomass (i.e., wood, i.e., *n* number of xylem cells of *x* dimensions: *sink limitation*) (Körner, 1998; Hoch *et al.*, 2002; Körner, 2003a; Hoch & Körner, 2005). Artificial warming likely stimulated an increase in respiration rates (Tjoelker, Reich & Oleksyn, 1999) and possibly an enhancement of the cell wall extensibility (i.e., changes in cell wall biochemistry) (Nakamura, Wakabayashi & Hoson, 2003), resulting in the production of wider and more hydraulically efficient xylem cells. Moreover, it seemed that the use of an increased amount of NSCs to build more and wider conduits was possible only around the heated zones, whereas the remaining portion of the stem at ambient temperature seemed to have received no stimuli to enhance xylogenesis.

This study may also be relevant within the context of predictions of global warming scenarios. Our findings support the hypothesis that increased growth rates of trees near the treeline and the treeline advance in altitude and latitude (Körner, 1998; Gamache & Payette, 2004; Harsch *et al*., 2009) are phenomena driven by the increase in atmospheric temperatures. Production of wider cells would certainly increase hydraulic efficiency of the transport system and stimulate tree growth. On the other hand, it would expose treeline trees to higher risks of xylem failure by cavitation after freeze-thaw cycles (Mayr *et al.*,

2003; Mayr *et al.*, 2006), thus compromising the survival success. Forecasting future scenarios of potential speed of further altitudinal and latitudinal treeline advance therefore remains a challenge.

In conclusion, this study essentially represents an extension of the *sink limitation hypothesis* (Körner, 1998; Hoch *et al.*, 2002; Körner, 2003a; Hoch & Körner, 2005): we analyzed the phenomenon of reduced height growth in trees at high altitude under a different perspective, that of hydraulic limitations. High altitude trees presented a xylem architecture optimally tapered to effectively compensate for the negative effect of height growth on the total hydraulic conductance, thus confining most of the resistance close to the stem apex (Yang & Tyree, 1993; Becker *et al.*, 2000; Petit *et al.*, 2008). Nevertheless, this hydraulic efficiency would allow for only small longitudinal increments because of the negative effect of cold temperatures on xylogenesis (Gričar *et al.*, 2006; Rossi *et al.*, 2007; Rossi *et al.*, 2008). In addition, any constraint to the xylogenesis around the stem apex would determine a negative effect on the whole tree hydraulics and, ultimately, on height growth.

The system used to carry on the experiment was in part developed by our department to provide a rugged, cost-effective system. The experience made in this work encouraged a further work to develop a real cost-effective integrated system for datalogging using open source hardware and software (see next chapter).

3 An effective datalogging system with Arduino

3.1 Introduction

The need for an economic and functional datalogging system to use in field experiments instead of our owned commercial solutions already in our possession, prompted me to work in the last year on the development of a cheap and functional product that could be lightweight, compact and fully customizable.

The choice to use Arduino (CC) instead of other microcontrollers available on the market come directly from my interest in Open Source Philosphy and Interaction Design (I could have my first Arduino skills attending an Interaction Design workshop in IUAV (Università di Venezia, Italy; Davide Rocchesso, Stephen Barrass: "The art of sonification, Interaction Design with Arduino").

Arduino is "an open-source electronics prototyping platform based on flexible, easy-to-use hardware and software. It's intended for artists, designers, hobbyists, and anyone interested in creating interactive objects or environments.
Arduino can sense the environment by receiving input from a variety of sensors and can affect its surroundings by controlling lights, motors, and other actuators. The microcontroller on the board is programmed using the Arduino programming language (based on the Wiring programming language) and the Arduino development environment (based on Processing). Arduino projects can be stand-alone or they can communicate with software on running on a computer (e.g. Flash, Processing, MaxMSP, PureData)." (see arduino.cc)

While the developing of our first prototype was on, the open-source community of developers and the "DIY" industries involved in same projects (Adafruit Industries) came to develop a dedicated "logshield" (a "shield" is a board that can be easily connected to the Arduino board and language) that could simplify

the necessary operations of a data logger (the reading of a clock signal from a RTC chip and storing the collected data on a media support such as an SD card with FAT16/32 filesystem) in just one board (instead of connecting different boards for each operation and using different software libraries for each board).

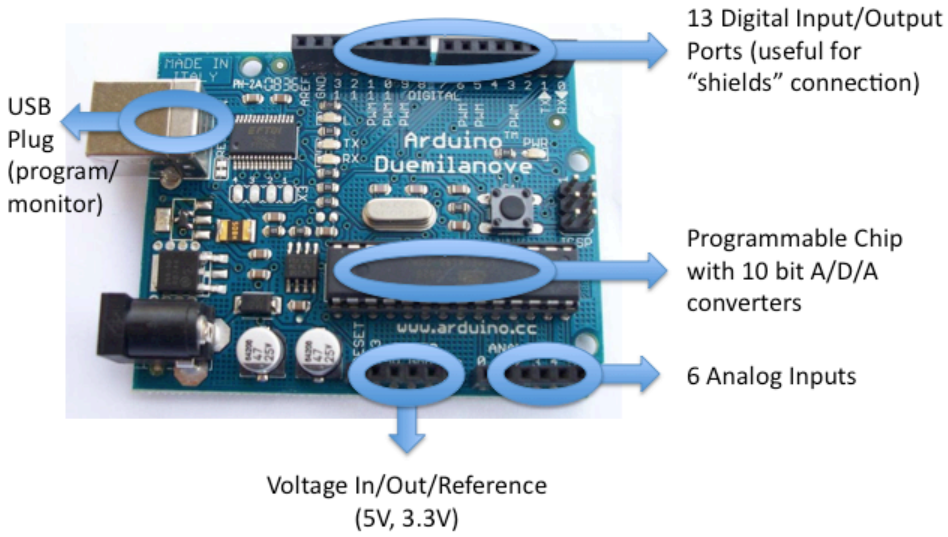

Fig. 3.1 Arduino Board (principal components highlighted). The picture scale is almost 1:1.

In a few months we passed from a prototype stage to a functioning product: I think that this is an example of the power of open-source and collaborating philosophy and I hope that money can be invested in future years to support these communities and their developers.
The stage of signal amplification was developed following the Granier system scheme, using high quality components (see 3.2).

The data is stored on a 2GB SD Card (which can provide space for years of datalogging) and can be easily downloaded also in field with any notebook equipped with a card reader. The enclosure is a rugged Gewiss-like box for electrical components. All contacts for sensors input, and SD card, are carried outside the box for convenience.

The Arduino (CC) team is: Massimo Banzi, David Cuartielles, Tom Igoe, Gianluca Martino, and David Mellis.

3.2 System Description

A digital datalogger is essentially a combo-unit composed of an Analog-to-Digital converter (ADC), a clock, and a controller board with a memory support for storing data. In our case, the data to be measured is a very small current voltage coming from a termocouple (see 3.3). To rescale the microVolt signal to a milliVolt scale we built a precision amplifier that is powered by the Arduino 5V output pin.

Data acquisition and log scheme:

- Signal amplifier: we built an high gain / low noise amplifier supplyed by a dual-12V/12V DC/DC voltage regulator chip (muRata NMA1212SC: 5 Volt to dual 12Volt) and a precision instrument amplifier (INA114AP) integrated chip for every signal input.
- Real Time Clock: the real time clock is the DS1307 chip which communicates with the Arduino Board using I2C protocol. It has a battery backup to keep the clock going for years even when the power supply of the board is off.

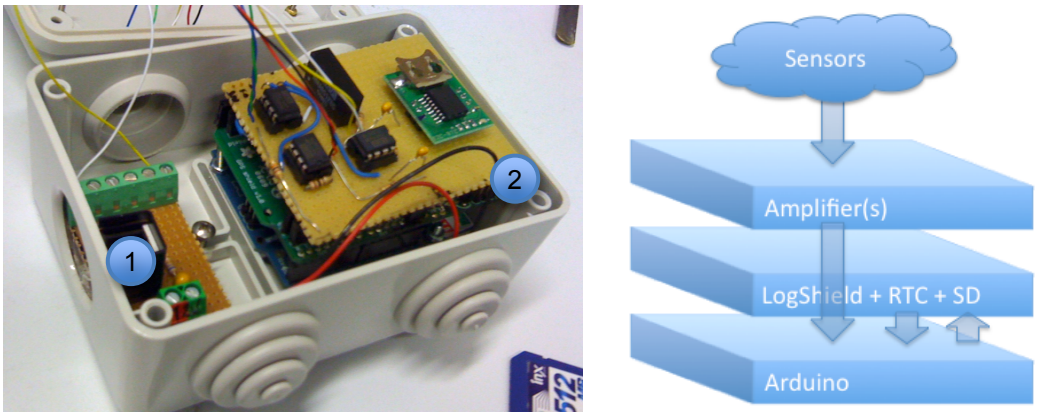

Fig. 3.2 Left image: the box contains: 1) the heating circuit for the "hot" probes of Granier Heat Dissipation Sap Flow measurement method (see next paragraph); 2) the data acquisition and log system, composed (as shown in the diagram in the Right image) by the Amplifier (the yellow board), and below it the LogShield and the Arduino Board (below all others). The signal follows the diagram on Right picture: from sensor probes, the signal goes to the amplifier, then is being converted into a digital 10 bit number from Arduino board; The Arduino board reads the clock from the LogShield and then stores the 10 bit number and the clock into the SD Card (which is in the LogShield board). Power supply (12V) comes from an outside battery or a solar panel.

- LogShield: the Adafruit Industries © LogShield board for Arduino is a board that fit perfectly the dimension of the Arduino Controller so that it can be connected very easily and also provide a bypass of many contacts of the Arduino Board. The LogShield is an integrated board which contains a Real Time Clock and the necessary to read/write a Fat 16/32 filesystem on a support such as a Secure Digital Memory Card (at the beginning of our project a GPS shield was used to store data on a memory suppord instead of this dedicated product). In our work we use 2 GB High Quality Class SanDisk SD Cards.

- Arduino Duemilanove board with ATMEL 328 chip: The ATMEL 328 chip is a programmable controller with 64K of internal memory to store the operating instructions; the chip is provided with 6 ADC converters with 10 bit precision and Pulse Width Modulation or Digital output ports; Arduino has also a FTDI chip to make it possible some monitoring functions on a serial communication via USB 2.0 protocol; The power supply can go from 9 to 20V (self scaling, with protection circuit) and it can be provided on a dedicated male-pin port, or via USB power supply. It is also possible to supply input voltage directly on board pins, and to set a Reference Tension (on the dedicated 'AREF' pin) to rescale the ADC converters. Reset button, and redundand ground connections are available for an easy prototyping of circuits.

3.3 First installations for sap flow measurement data log

In summer 2010, Prof. T. Anfodillo and M. Carrer took part in the FUNCiTREE project and carried four of our dataloggers to Nicaragua and Costa Rica, in collaboration with Fabrice DeClerk of CATIE (Centro Agronómico Tropical de Investigación y Enseñanzaed - Turrialba, Costa Rica).
To measure the transpiration of the trees they used the Granier method, introduced by A. Granier in 1985. The Heat Dissipation method for sap flow measurement (Granier 1985; Granier 1987 a,b) consists of two termocouple

probes strung pretty close toghether into the tree trunk which are used for a differential reading of temperature.
One of the probes is heated by a resistive circuit (see fig. 3.3): this is necessary to radiate a temperature into the trunk making it possible to read the temperature difference between this "hot" termocouple and the other probe (the "cold" one) that is used as reference.

The making of the two probes is quite easy and affordable for all, so we have built by us. A good construction guide is the one shown in this web page:
http://www.cens.ucla.edu/pub/EnvironmentalSolutions/Sapflow_Tutorial.html,
but instead of soldering the two copper and constantane wires as shown in the CENS-UCLA guide, we used a fine wire welder to obtain termocouples of higher quality.

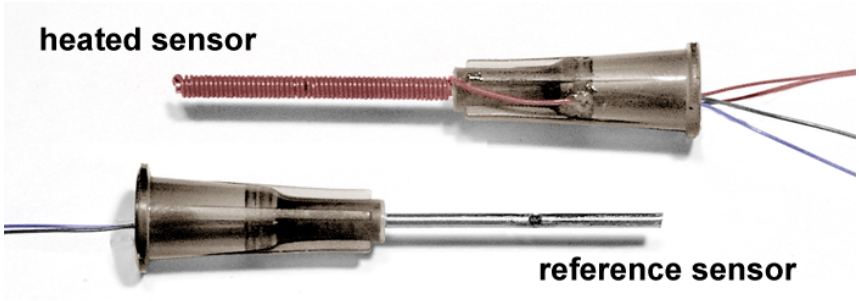

Fig. 3.3 Heat dissipation sap flow probes: Inside the needle it is placed a termocopule made of copper and constantane wire; in the "heated sensor" you can see the coil of resistive wire used to radiate heat. Instead of soldering the two wires inside the needle, we used a Fine Wire Welder, (MODEL: J60M - LAB FACILITY LTD) to obtain a more affordable and high-quality termocouple.

The length of our probes (10 mm) is less than that in the original Granier system (20 mm) because if the probes are shorter they are also easier to build, and the flow measurement is not affected by their length (Philips "Sacred Sap Flow Package" - Boston University).
The heating of the hot probe is carried out with a current of 120 milliAmps which corresponds to a dissipation of about 0.1 Watt for a 10 mm probe. The power

supply is given by a 12 Volt battery (which also supplies the data logger) or a solar panel (of about 1 square meter).

With this method and characteristics, we read a maximum temperature difference of 12.5°C when the flow is zero. To convert between the difference of temperature (deltaT) of the probes and sap flow, there's an empirical formula (Granier 1985):

$$\text{SapFlow} = 4.284 \cdot \left(\frac{deltaT_{MAX}}{deltaT} - 1 \right)^{1.231} \quad \left[\frac{dm^3}{dm^2} / h \right]$$

To avoid an unwanted heating of the trunk due to sun radiation, with a consequent impairment of the measure of the temperature difference, the whole area in which sensors are placed, is surrounded with TermoFlex material. (see fig. 3.4)

Fig. 3.4 Installation of Granier probes in two different sites. Left image: Pontedera, Pisa - Italy: It is visible the TermoFlex used to prevent the heating of the trunk due to solar radiation. Right image: CATIE - FUNCiTREE project, Costa Rica: probes are being inserted into a tree trunk.

3.4 Data acquired

Despite the interest in collecting transpiration data, the first installations we have done had the main purpose of testing the strenght of our system in real conditions (before these installations we just had laboratory tests) for the acquisition of field data and durability of the hardware and software.

We could made two very different sites of installations. The first installation was made on tropical plants in CATIE (Rurrialba, Costa Rica), and it is still working, the other installation was made on young trees of *Populus x euramericana clone I-214* and *Populus x generosa x Populus nigra* in Pontedera (Pisa, Italy) in collaboration with the Scuola di Studi Superiori Sant'Anna of Pisa, ref. Luca Sebastiani, and it has been removed at the end of summer season.

In the first site, Nicaragua, we had no problems for data acquisition and environmental factors (except for the unfortunate theft of two loggers) and after some months we have results that confirm the correct functioning of the datalog system (see fig 3.5).

Unfortunately, in the Pontedera site we had a serious problem with the power supply of the system that has stopped the acquisition of data beyond a certain

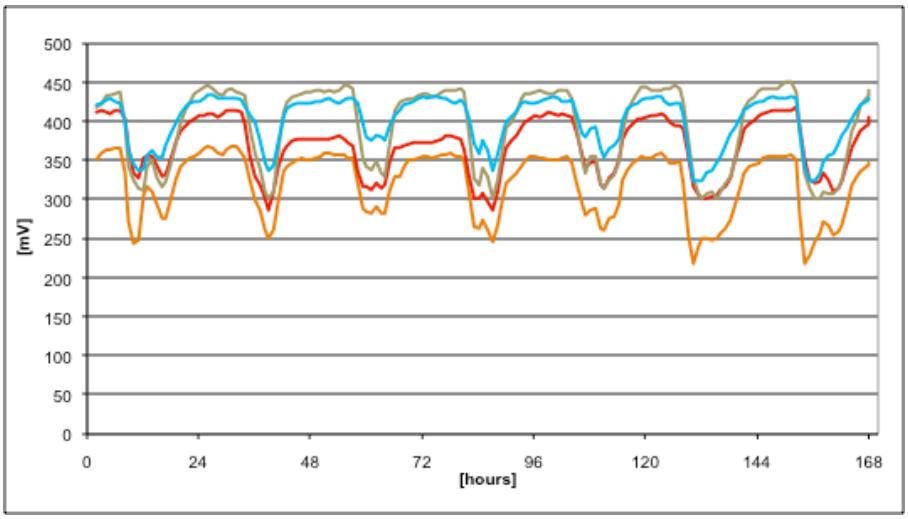

Fig. 3.5 Example of weekly transpiration log of for some of the plants (one tree, one color) in CATIE, Costa Rica. The raw data showed come directly from the Analog to Digital conversion State of the Arduino logger. It is possible to see that there are no big gaps in the data acquisition and that the signal follows the tipical trend of daily transipration.

date (probably the date of a lightning strike; or the day of a possible failure of the stabilized power supply unit.).

In this second site, the arduino overvoltage protection chip, the voltage regulator, and also the power supply chip of signal amplifier were literally melted. Also the heating circuit of the Granier Heat Dissipation Sensors System was partly burned. This lead us to suppose the sudden arrival of a voltage much higher than the maximum manageable from the Arduino board, that is 20V. Despite this overload problem, we could collect from the SD Card a month of data acquired, which also confirms the correct operation of the datalogger throughout the period before the accident (see fig 3.6)

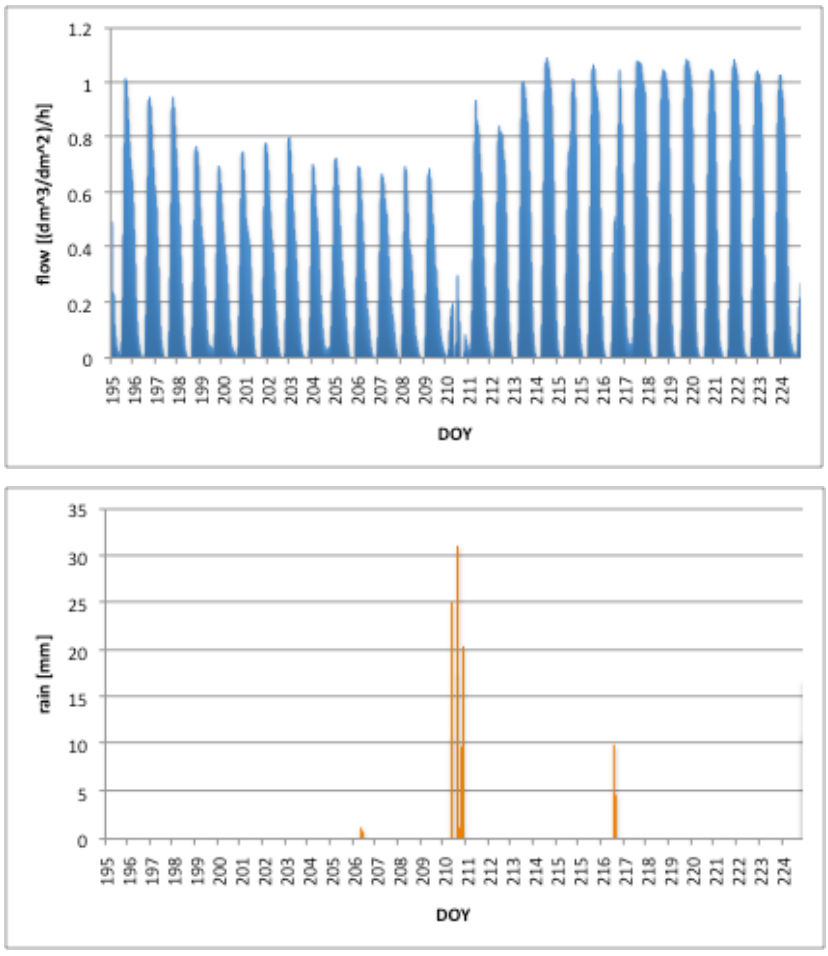

Fig. 3.6 Image on top: Sap flow measures (horizontal axis goes from july 14th to august 11th, 2010) after the day 210-211 see a greater transpiration of the plant examined. In the image below are shown the precipitation data that confirms an heavy rainfall on days 210-211 which made available a greater hydration of the land for the next days.

3.4 The Arduino Code

This is the PDE code to program the Arduino Board for datalogging and serial monitoring; we calibrated it for convenience to scale the reading of milliVolt from probes to the same scale we had when using Campbell's CR10X datalogger.
The code is released under Creative Commons 3.0 CC-BY-NC, which means that everybody is free to share, remix, tweak, and build upon their work non-commercially, by attribution to this PhD Thesis. Although the new works coming from this code must also acknowledge this license and be non-commercial. They also don't have to license their derivative works on the same terms.
To set correctly the DS1307 Real Time Clock, any code inside the RTCLib Arduino Example is fine.
The software Libraries used in this work are listed in the code. In case of using the Adafruit Logshield a comprensive tutorial and collection of necessary libraries and skills is available on the web, on www.ladyada.net

```
1  // With this code we log 3 sensors, on Analog Input PIN 1,2,3
2  #define LOG_INTERVAL  5000 // mills between entries
3  #define SENSOR_COUNT     4 // number of analog pins to log
4  #define ECHO_TO_SERIAL   1 // echo data to serial port
5  #define WAIT_TO_START    1 // Wait for serial input in setup()
6  #define SYNC_INTERVAL 1000 // mills between calls to sync()
7  #define Binary 0
8  #define Hex 1
9  uint32_t syncTime = 0;     // time of last sync()
10
11 #include <Wire.h>
12 #include "Fat16.h"
13 #include "SdCard.h"
14 SdCard card;
15 Fat16 file;
16
```

```
17  /*********************************************************************************
18   * Function Prototype
19   *********************************************************************************/
20  unsigned int SerialNumRead (byte);
21  void SetTime();
22  void DisplayTime();
23
24  void error(char *str)
25  {
26
27    Serial.print("error: ");
28    Serial.println(str);
29    while(1);
30  }
31
32  /*********************************************************************************
33   * Global variables
34   *********************************************************************************/
35  const int I2C_address = 0x68;  // I2C write address
36  byte    Second;     // Store second value
37  byte    Minute;     // Store minute value
38  byte    Hour;       // Store hour value
39  byte    Day;        // Store day value
40  byte    Date;       // Store date value
41  byte    Month;      // Store month value
42  byte    Year;       // Store year value
43  int     counter  =  0;
44
45  /*********************************************************************************
46   * Setup
47   *********************************************************************************/
48  void setup()
49  {
50    Serial.begin(9600);
51    Wire.begin();        // join i2c bus (address optional for master)
52  /*  delay(1000);
```

```
#if WAIT_TO_START
  Serial.println("Type any character to start");
  while (!Serial.available());
#endif //WAIT_TO_START
*/
  // initialize the SD card
  if (!card.init()) error("card.init");

  // initialize a FAT16 volume
  if (!Fat16::init(card)) error("Fat16::init");

  // create a new file
  char name[] = "LOGGER00.CSV";
  for (uint8_t i = 0; i < 100; i++) {
    name[6] = i/10 + '0';
    name[7] = i%10 + '0';
    if (file.create(name)) break;
  }
  if (!file.isOpen()) error ("file.create");
  Serial.print("Logging to: ");
  Serial.println(name);

 // write header
  file.print("date,time");
  Serial.print("date,time");

  file.writeByteError = 0;
/*  file.print("millis");
#if ECHO_TO_SERIAL
  Serial.print("millis");
#endif //ECHO_TO_SERIAL
*/

    file.print(",sensor1,sensor2,sensor3");
    Serial.print(",sensor1,sensor2,sensor3");
    file.println();
```

```
89      Serial.println();
90
91    if (file.writeByteError || !file.sync()) {
92      error("write header");
93    }
94  }
95
96  /*****************************************************************************
97   * Main Loop
98   *****************************************************************************/
99
100 void loop()
101 {
102   boolean Readtime;       // Set/Read time flag
103   unsigned int Incoming;  // Incoming serial data
104   counter++;
105
106   // clear print error
107   file.writeByteError = 0;
108   delay((LOG_INTERVAL -1) - (millis() % LOG_INTERVAL));
109
110   // Log Time RTC
111   DisplayTime();
112
      // la lettura è fatta ogni 5 secondi e stampata alla porta seriale. Ogni 60secondi è invece registrata
113 su SD.
114   uint16_t data1 = analogRead(1);
115   uint16_t data2 = analogRead(2);
116   uint16_t data3 = analogRead(3);
117   if (counter==12)  {
118     file.print(data1*(4.88758/5));
119     file.print(',');
120     file.print(data2*(4.88758/5));
121     file.print(',');
122     file.print(data3*(4.88758/5));
123     file.print(',');
```

```
124     file.println();
125     counter = 0;
126   }
127 #if ECHO_TO_SERIAL
128     Serial.print(data1*(4.88758/5));
129     Serial.print(',');
130     Serial.print(data2*(4.88758/5));
131     Serial.print(',');
132     Serial.print(data3*(4.88758/5));
133     Serial.print(',');
134     Serial.println();
135 #endif
136
137   if (file.writeByteError) error("write data");
138
139   //don't sync too often - requires 2048 bytes of I/O to SD card
140   if ((millis() - syncTime) <  SYNC_INTERVAL) return;
141   syncTime = millis();
142   if (!file.sync()) error("sync");
143   //Serial.print('#');
144
145 }
146
147
148 /*******************************************************************************
149  * Display time function
150  *******************************************************************************/
151 void DisplayTime()
152 {
153   char tempchar [7];
154   byte i = 0;
155   Wire.beginTransmission(I2C_address);
156   Wire.send(0);
157   Wire.endTransmission();
158
159   Wire.requestFrom(I2C_address, 7);
```

```
160
161   while(Wire.available())         // Checkf for data from slave
162   {
163     tempchar [i] = Wire.receive(); // receive a byte as character
164     i++;
165   }
166   Second = tempchar [0];
167   Minute = tempchar [1];
168   Hour   = tempchar [2];
169   Day    = tempchar [3];
170   Date   = tempchar [4];
171   Month  = tempchar [5];
172   Year   = tempchar [6];
173
174   // Display time
175  //  Serial.print("The current time is ");
176   Serial.print(Month, HEX);
177   Serial.print("/");
178   Serial.print(Date, HEX);
179   Serial.print("/20");
180   if (Year<10)
181     Serial.print("0");
182   Serial.print(Year, HEX);
183   Serial.print(",");
184   Serial.print(Hour, HEX);
185   Serial.print(".");
186   Serial.print(Minute, HEX);
187   Serial.print(".");
188   Serial.print(Second, HEX);
189   Serial.print(",");
190   // Log Time to SD
191  //  file.print("The current time is ");
192   if  (counter==12) {
193   file.print(Month, HEX);
194   file.print("/");
195   file.print(Date, HEX);
```

```
196     file.print("/20");
197     if (Year<10)
198       file.print("0");
199     file.print(Year, HEX);
200     file.print(",");
201     file.print(Hour, HEX);
202     file.print(".");
203     file.print(Minute, HEX);
204     file.print(".");
205     file.print(Second, HEX);
206     file.print(",");
207     }
208   }
```

3.4 Discussion

The interesting thing to note in the case of the accident happened to the Pisa site is that the costs to repair such a damage are below 100$ since the Arduino board and the burned components have a total commercial value not exceeding 50$, and the time needed to replace the burned parts and reprogramming the Arduino board is about one hour or two.

Of course the costs of a commercial solution are higher, and the flexibility of the system is lower; our system has the advantage to be economic, small, easy to repair, disassemble, rebuild, reprogram and modify. The data being measured and logged can be monitored in every moment with the USB connection, and if the datalogger stops to work for blackout or external problems, a new file is made to make the gap immediatly visible when the files are downloaded from the SD card.

Fig. 3.7 Picture of the dataloggers. The input and output contacts of the probes, and the SD Card Slot are outside the box for convenience.

4 Discussion and Conclusions

As an engineer, a vast part of my work has been to figure out how a tree "works" and what are the factors that may limit its growth in many way; probably for this reason the works on which I was able to focus during my PhD are numerous and not all reportet in this Thesis; some of them have been quite different from each other, despite the common thread to try to understand why trees stop growing in height. In conclusion, I could have the opportunity to develop a path that contained both modeling work and applied work.

The first part of the work presented in this Thesis highlighted the fundamental importance of the tapering of xylem conduits in the logic of an optimized transport of resources inside the trees. This hypothesis proposed in the context of the WBE model (West, Bronw and Enquist, 1997 and 1999) is compatible with the minimization criterion proposed by the BMR model (Banavar, Maritan, Rinaldo 1999), and the combination of both models generates a degree of tapering compatible with that measured in real trees, assuming that is represents an optimal value achieved when the plant is at the limits of its possibilities for growth.

The experiment presented in the second part confirms that the hydraulic efficiency of the xylem architecture represents a relevant limiting factor for height growth at high altitude, and our work confirmed that the dimension of apical conduits and the degree of tapering are the two most important features of the xylem anatomy, in particular the dimension of apical conduits and the degree of tapering, which was demonstrated as the most effective mechanism of compensation for the increase in hydraulic resistance with increasing path length (i.e., tree height). The conducting of this experiment gave then to me the idea to think about the opportunities of having a system for data acquisition that could only rely on the skills of our department. This gave me the opportunity to build and test an almost-free new system for data logging, and to test it for sap flow measurements in two field experiments, confirming the possibilities of this new solution.

References

Anderson G & Bancroft J (2002) Tissue processing and microtomy including frozen. In: J. Bancroft & J.D. Gamble, eds. Theory and Practice of Histological Techniques (eds.), London, UK: Churchill Livingstone, 87-107.

Anfodillo T, Carraro V, Carrer M, Fior C & Rossi S (2006) Convergent tapering of xylem conduits in different woody species. New Phytologist 169: 279-290.

Banavar J, Maritan A, Rinaldo A (1999) Size and form in efficient transportation networks. Nature (1999) 399, 130-132

Becker P, Gribben RJ & Lim CM (2000) Tapered conduits can buffer hydraulic conductance from path-length effects. Tree Physiology 20: 965-967.

Coomes DA (2006) Challenges to the generality of WBE theory. Trends in Ecology and Evolution 21: 593-596.

Coomes DA & Allen RB (2007) Effects of size, competition and altitude on tree growth. Journal of Ecology 95: 1084-1097.

Coomes DA, Jenkins KL & Cole LES (2007) Scaling of tree vascular transport system along gradients of nutrient supply and altitude. Biology Letters 3: 86-89.

Danby RK & Hik DS (2007) Responses of white spruce (*Picea glauca*) to experimental warming at a subarctic alpine treeline. Global Change Biology 13: 437-451.

Davison AC & Hinkley DV (1997) Bootstrap Methods and their Applications. New York: Cambridge University Press.

Gorsuch DM & Oberbauer SF (2002) Effects of mid-season frost and elevated growing season temperature on stomatal conductance and specific xylem conductivity of the arctic shrub, *Salix pulchra*. Tree Physiology 22: 1024-1037.

Granier A (1985) Une nouvelle méthode pour la mesure du flux de sève brute dans le tronc des arbres. Annales des Sciences Forestières 42:193-200.

Granier A (1987a) Mesure du flux de se`ve brute dans le tronc du Douglas par une nouvelle me´thode thermique. Annales des Sciences Forestie`res 44, 1–14.

Granier A (1987b) Evaluation of transpiration in a Douglas-fir stand by means of sap flow measurements. Tree Physiology 3, 309–320.

Gričar J, Zupančič M, Čufar K, Koch G, Schmitt U & Oven P (2006) Effect of local heating and cooling on cambial activity and cell differentiation in the stem of Norway spruce (*Picea abies*). Annals of Botany 97: 943-951.

Harsch MA, Hulme PE, McGlone MS, Duncan RP. 2009. Are treelines advancing? A global meta-analysis of treeline response to climate warming. Ecology Letters 12: 1040-1049.

Hoch G, Popp M & Körner C (2002) Altitudinal increase of mobile carbon pools in *Pinus cembra* suggests sink limitation of growth at the Swiss treeline. OIKOS 98: 361-374.

Hoch G, Körner C. 2005. Growth, demography and carbon relations of Polylepis trees at the world's highest treeline. Functional Ecology 19: 941-951.

Jalkanen R, Tuovinen M (2001) Annual needle production and height growth: better climate predictors than radial growth at treeline?. Dendrochronologia 19: 39–44.

Kleiber M (1932) "Body size and metabolism". Hilgardia 6: 315–351.

Kozlowski J & Konarzewski M (2004) Is West, Brown and Enquist's model of allometric scaling mathematically correct and biologically relevant? Functional Ecology 18: 283-289.

Körner C (1998) A re-assessment of high elevation treeline position and their explanation. Oecologia 115: 445-449.

Körner C (2003) Alpine Plant Life - Functional Plant Ecology of High Mountain Ecosystems. Heidelberg: Springer.

Makarieva AM, Gorshkov VG & Li BL (2005) Revising the distributive networks models of West, Brown and Enquist (1997) and Banavar, Maritan and

Rinaldo (1999): Metabolic inequity of living tissues provides clues for the observed allometric scaling rules. Journal of Theoretical Biology 237: 291-301.

Mandelbrot B (1982) The Fractal Geometry of Nature. San Francisco: Freeman.

Mayr S, Hacke U, Schmid P, Schwienbacher F, Gruber A. 2006. Frost drought in conifers at the alpine timberline: xylem dysfunction and adaptations. Ecology 86: 3175-3185.

Mayr S, Cochard H, Améglio T, Kikuta SB. 2007. Embolism formation during freezing in the wood of Picea abies. Plant Physiology 143: 60-67.

Mencuccini M, Martínez-Vilalta J, Hamid HA, Korakaki E & Vanderklein D (2007) Evidence for age- and size-mediated controls of tree growth from grafting studies. Tree Physiology 27: 463-473.

Mencuccini M, Hölttä T, Petit G & Magnani F (2007) Sanio's law revisited. Size-dependent changes in the xylem architecture of trees. Ecology letters

Petit G (2007) analysis of the tapering of xylem conduits as a compensation mechanism for hydraulic limitations to tree growth. Tesi di Dottorato in Scuola TARS, Università degli Studi di Padova, Padova, Italy.

Petit G, Anfodillo T (2009) Plant physiology in theory and practice: an analysis of the wbe model for vascular plants. Journal of Theoretical Biology, 259 (2009) 1–4

Petit G, Anfodillo T, De Zan C. 2009. Degree of tapering of xylem conduits in stems and roots of small Pinus cembra and Larix decidua trees. Botany 87: 501-508.

Petit G, Anfodillo T & Mencuccini M (2008) Tapering of xylem conduits and hydraulic limitations in sycamore (*Acer pseudoplatanus*) trees. New Phytologist 177: 653-664.

Petit G, Anfodillo T, Carraro V, Grani F, Carrer M (2010) Hydraulic constraints limit height growth in trees at high altitude. New Phytologist (2010) Vol 189, Issue 1, pages 241-252, January 2011 - doi: 10.1111/j.1469-8137.2010.03455.x.

Roberntz P. 1999. Effects of long-term CO2 enrichment and nutrient availability in Norway spruce. I . Phenology and morphology of branches. Trees 13: 188-198.

Riondato R (2009) Xilogenesi ed accrescimento longitudinale al limite superiore del bosco: determinanti ambientali e fisiologici. Tesi di Dottorato in Scuola TARS, Università degli Studi di Padova, Padova, Italy.

Rossi S, Deslauriers A, Anfodillo T & Carraro V (2007) Evidence of threshold temperatures for xylogenesis in conifers at high altitude. Oecologia 152: 1-12.

Rossi S, Deslauriers A, Anfodillo T, Carrer M. (2008). Age-Dependent Xylogenesis In Timberline Conifers. NEW PHYTOLOGIST, vol. 177; p. 199-208, ISSN: 0028-646X

Sokal RR, Rohlf FJ. 1981 Biometry. New York, USA: W.H. Freeman.

Sperry JS, Nichols KL, Sullivan JE & Eastlack M (1994) Xylem embolism in ring porous, diffuse porous and coniferous trees of northern Utah and interior Alaska. Ecology 75: 1736-1752.

Sperry JS, Hacke UG & Wheeler JK (2005) Comparative analysis of end wall resistivity in xylem conduits. Plant, Cell and Environment 28: 456-465.

Weitz JS, Ogle K & Horn HS (2006) Ontogenetically stable hydraulic design in woody plants. Functional Ecology 20: 191-199.

West GB, Brown JH & Enquist BJ (1997) A general model for the origin of allometric scaling laws in biology. Science 276: 122-126.

West GB, Brown JH & Enquist BJ (1999) A general model for the structure and allometry of plant vascular systems. Nature 400: 664-667.

Zimmermann MH (1978) Hydraulic architecture of some diffuse-porous trees. Canadian Journal of Botany 56: 2286-2295.

Zimmermann MH (1983) Xylem Structure and the Ascent of Sap. New York, USA: Springer-Verlag.

Yang S, Tyree MT. 1993. Hydraulic resistance in Acer saccharum shoots and its influence on leaf water potential and transpiration. Tree Physiology 12: 231-242.